scientific reports

Check for updates

OPEN

# Differential expression of reproduction and sex-determining genes in the gonads of genotypic and temperature-induced males of gibel carp (*Carassius gibelio*)

Florian Jacques[1]✉, Lukáš Vetešník[1,2], Iva Dyková[1], Nicolas Blavet[3] & Andrea Šimková[1,4]✉

**Sex in vertebrates is commonly determined by genotype and environmental conditions, such as temperature. A few species display intermediate systems, combining sex chromosomes with temperature effect. This phenomenon has been reported in gibel carp (*Carassius gibelio*), an invasive cyprinid fish whose invasiveness is linked to the combination of sexual and asexual reproduction. Here, we compared gonadal transcriptomes between genotypic males and temperature-induced males of *C. gibelio*, focusing specifically on genes related to reproduction. Many meiosis and male differentiation pathways were common to genotypic and temperature-induced males. However, the underrepresentation of reproduction- and spermatogenesis-related terms in temperature-induced males suggests reduced reproductive abilities. Our study further highlights differential regulation of key genes related to male differentiation, steroid hormone signalling, meiosis, spermatogenesis, flagellar function, and sperm-egg interaction. In particular, induced males strongly overexpressed the key sex differentiation regulator *hsd17b2* and slightly overexpressed the meiotic gene *mnd1*, while genotypic males overexpressed *sox8a*, *cyp19a1a*, and the crucial fertilization gene *izumo*. Our study highlights the importance of males in the transition from asexual to sexual reproduction in this species and contributes to understanding the molecular mechanisms underlying the reproductive plasticity and invasiveness of *C. gibelio* in Europe.**

**Keywords** *Carassius gibelio*, Transcriptomics, Differential gene expression, Meiosis-associated pathways, Genotypic sex differentiation, Temperature sex differentiation

In gonochoristic species, sex is determined by sex chromosomes in the case of genotypic sex determination (GSD), or by environmental conditions, such as temperature (temperature-dependent sex determination, or TSD)[1,2], photoperiod[3], social factors[4,5], water pH or oxygen availability[6–8]. The main GSD systems include the male heterogametic XY system and its variant X0, and the female heterogametic ZW system[1,2]. In fish, while TSD is rare compared to GSD[9], it has been reported in dozens of species, such as *Menidia menidia*[10], *Hoplosternus littorale*, *Odontesthes argentinensis*, *Limia melanogaster*, *Poeciliopsis lucida*, and species of the *Apistogramma* genus[9]. However, different sex determination mechanisms can act in the same species[2,9,11], and environmental modulation of sex ratio in species with GSD is common[2,12]. For example, the effect of temperature on sex determination is reported in the model cyprinid fish *Danio rerio*, which has the ZW sex determination system combined with sex-linked single nucleotide polymorphism (SNP)[13]. The effect of temperature on species with GSD was also reported in *Menidia*[10], *Carassius auratus* and *C. carassius*[9]. Hence, multiple intermediate states between GSD and strict TSD exist, and GSD and TSD have been proposed as the two ends of a continuum[14]. In both GSD and TSD species, sex determination relies on the activation of specific genes. For example, *sry* of the Y chromosome is a major male-determining gene in mammals (for review, see Waters et al[15].). Inversely, *cirbp*

[1]Department of Botany and Zoology, Faculty of Science, Masaryk University, Kotlářská 2, Brno 611 37, Czech Republic. [2]Institute of Vertebrate Biology of the Czech Academy of Sciences, Květná 8, Brno 603 65, Czech Republic. [3]Central European Institute of Technology, Masaryk University, Brno 625 00, Czech Republic. [4]Faculty of Fisheries and Protection of Waters, University of South Bohemia in České Budějovice, South Bohemian Research Center of Aquaculture and Biodiversity of Hydrocenoses, Zátiší 728/II, Vodňany 389 25, Czech Republic. ✉email: florian.jacques@sci.muni.cz; simkova@sci.muni.cz

has been proposed to be specifically related to TSD in the turtle *Chelydra serpentina*[16]. In fish with GSD, male-determining genes include *dmy*, identified in the model teleost medaka (*Oryzias latipes*)[17], a Y chromosome duplicate of *amh* (encoding the anti-Müllerian hormone) in the Nile tilapia (*Oreochromis niloticus*)[18], and the highly conserved *dmrt1* gene in teleosts[19].

The gibel carp (*Carassius gibelio*) is a cyprinid fish species that originated in eastern Eurasia and colonized European freshwater ecosystems in the 1970s. The species is now widely distributed and considered invasive in Europe, competing with native local cyprinids – especially the crucian carp (*Carassius carassius*)[20–24]. The gibel carp is a member of the *Carassius auratus* complex, and likely originates from the diploid *C. auratus* via triploidization around 0.5 million years ago[25,26]. The first European populations of gibel carp were composed of triploid females only, which reproduced using gynogenesis, an asexual reproduction mode where the eggs are only activated by sperm, with no genetic contribution of sperm to the offspring.

In contrast to most unisexual species[27,28], sexual reproduction and males also exist in *C. gibelio* populations. Male proportions in these populations vary between 0 and 45%. Males are mostly diploid, but triploid and tetraploid males are also occasionally present[29]. Some species of the *Carassius* genus combine the male heterogametic (XY) sex determination system[30] with an effect of temperature on sex differentiation[9,31]. Cold and heat treatments induce sex reversal in genotypically female fish larvae[32]. Hence, GSD and TSD males coexist in *C. gibelio* populations, but although GSD and TSD males exhibit similar external morphology, testis histology, and sperm structure and vitality, significant functional differences have been reported[33]. Notably, sperm from TSD males are unable to fuse with the female pronucleus, and fertilized eggs with TSD sperm show an absence of nuclear replication. Moreover, TSD males display defects in DNA replication and dysregulation of genes related to the cell cycle, transcription, and translation when compared with GSD males[33]. These findings suggest that temperature not only induces male development but also disrupts key molecular processes underlying male gamete function[33].

Furthermore, like around 15% of eukaryotic species[34], *C. gibelio* is characterized by the presence of male-specific supernumerary B chromosomes, or microchromosomes with non-Mendelian inheritance, which combine homologous sequences of autosomes and abundant repetitive elements[35], as well as transposable elements. Microchromosomes were shown to play a role in male determination in gynogenetic *C. gibelio*[36], in a way similar to sex chromosomes and male-specific genetic elements. Hence, they were proposed to be the main driving force underlying male occurrence in *C. gibelio*[35], and may have played a role during the evolutionary transition from unisexual to sexual reproduction in polyploid fish[34]. Since asexual reproduction lacks genetic mixing and leads to the accumulation of deleterious mutations[37], the maintenance of sex and males in *C. gibelio* favors genetic diversity and adaptive abilities, particularly in the immune response to pathogens[38,39], and counterbalances the effect of Müller's ratchet[40]. Hence, the high ecological tolerance and adaptive abilities of *C. gibelio* could result from the combination of sexual reproduction and gynogenesis[41].

The complex population structure of *C. gibelio* makes this species unique to investigate the re-appearance of males in unisexual forms, and the mechanisms of female-to-male switches in nature. *Carassius gibelio* also represents a transitional state between unisexual and bisexual reproduction. Therefore, this unique system is suitable for investigating the transition between different sex determination systems. Full transcriptome comparisons are critical for understanding how reproduction-associated pathways are modulated in species that combine genetic and environmental mechanisms of sex determination. So far, only a few attempts have been made to systematically compare transcriptomic differences between GSD and TSD males of the same species. However, although several potential gonadal temperature-sensitive genes have been identified by transcriptome study[42], the molecular mechanisms underlying TSD remain poorly characterized. Studies on Nile tilapia suggest that critical sex-determination genes, including *dmrt1*, *gsdf*, and *gadd45* are differentially regulated under high-temperature sex induction[43]. Furthermore, genes involved in cell cycle control, meiosis, and homologous recombination have been implicated in temperature-driven sex differentiation[44].

In this study, we tested the effect of temperature on the expression of the male phenotype of gynogenetic *C. gibelio*. Using transcriptome profiling of testes tissues, we analyzed the differential expression of sex determination genes and reproduction-associated genes in genetically determined diploid males obtained by crossing sexual diploid females and males, and in temperature-induced triploid males generated by exposing gynogenetic triploid females to different temperature treatments. We also compared transcriptomes from testes under different sex determination regimes - high temperature induction only, both low and high temperature induction, and genotypic sex determination. To our knowledge, this represents the first attempt to examine transcriptomic variation across both low-temperature and high-temperature TSD systems in contrast with GSD. We hypothesized that the expression of reproduction-associated genes differs between genetically determined and temperature-induced males, and between different systems of TSD (low and high TSD, or high TSD only). Moreover, we specifically focused on genes previously reported to be involved in sex determination, such as *amh*, *sf1* and members of the *sox*, *gsdf* and *dmrt* families. Through these comparisons, we attempted to identify several potential gonadal temperature-sensitive genes, providing new insights into the processes of environmental sex determination. Our findings advance the understanding of TSD mechanisms in fish with genotypic sex determination and shed light on how environmental factors regulate sex control in invasive species.

## Results

Sex ratio of the offspring of sexual diploid gibel carp (genotypic offspring) was 1:1. Two outputs associated with production of males during gynogenesis were found: (1) a triploid gynogenetic female produced only female offspring at 22 °C, a low proportion (20–30%) of male offspring at 25 °C (observed only when males of *Cyprinus carpio* or *C. gibelio* were used for egg activation, while using sperm from *Abramis brama* resulted in fat tissue development instead of formation of male gonads), and only male offspring at 28 and 31 °C (full sex reversal

induced by high temperature); or (2) a triploid gynogenetic female produced offspring with 70–85% males already at 22 °C, 80–100% males at 25 °C, and 100% males (full sex reversal) at 28 and 31 °C.

## Gonadal histology

Genotypic diploid males from the wild ($n$ = 6): Seminiferous tubules containing mainly spermatozoa as dominant spermatogenic stage throughout their entire length were lined with a thin discontinuous layer of germinal epithelium (Fig. 1a, c). They were assigned to the 'spent' stage of the reproductive cycle[45]. One male of this group, showing all stages of spermatogenesis in the seminiferous tubules, was assigned to the 'maturation' class. Triploid males from the wild ($n$ = 6): predominant signs characteristic of the "spent" reproductive class, with discontinuous germinal epithelium lining the seminiferous tubules filled with masses of spermatozoa were found in 5 of the 6 males examined (Fig. 1b). Spermatocytes and spermatids were scattered in a small number of seminiferous tubules. All spermatogenic stages were observed in only one individual.

Genotypic diploid males from artificial breeding ($n$ = 6): All spermatogenesis stages were present in five of the six males examined. Due to the predominance of spermatocysts containing spermatogonia, spermatocytes, spermatids, and fewer spermatozoa in the seminiferous tubules and ducts, these fish were assigned to the intermediate maturation class of reproduction (Fig. 2a). Temperature-induced triploid males from artificial breeding ($n$ = 6): All stages of spermatogenesis were found, but spermatozoa were less abundant than in genotypic diploid males, i.e., this group belonged to the early maturation reproductive class (Fig. 2b, c). The testes of all individuals examined histologically contained spermatozoa in seminiferous tubules and ducts (Figs. 1 and 2). No individuals were immature or showed regressed testes. Histology-based reproductive classification assessed genotypic diploid and induced triploid males as capable of spawning and assigned them to the maturing or spent classes irrespective of their origin. Detailed conditions of spermatogenic stages could not be determined.

## Differential expression analysis

A total of 9696 genes were differentially expressed between genotypic diploid and temperature-induced triploid males of *C. gibelio*. Among them, 4987 genes were more highly expressed in temperature-induced males, and 4709 were more highly expressed in genotypic males (hierarchical clustering of specimens based on the top 2000 DEG is shown in Fig. 3). PCA based on transcriptome-wide gene expression (Fig. 4A) showed differences in transcriptome profiles between genotypic and induced males which were separated along PC1. No confounding factors from the DESeq2 model were found using the PCA. The three groups of induced males, i.e., sex reversal

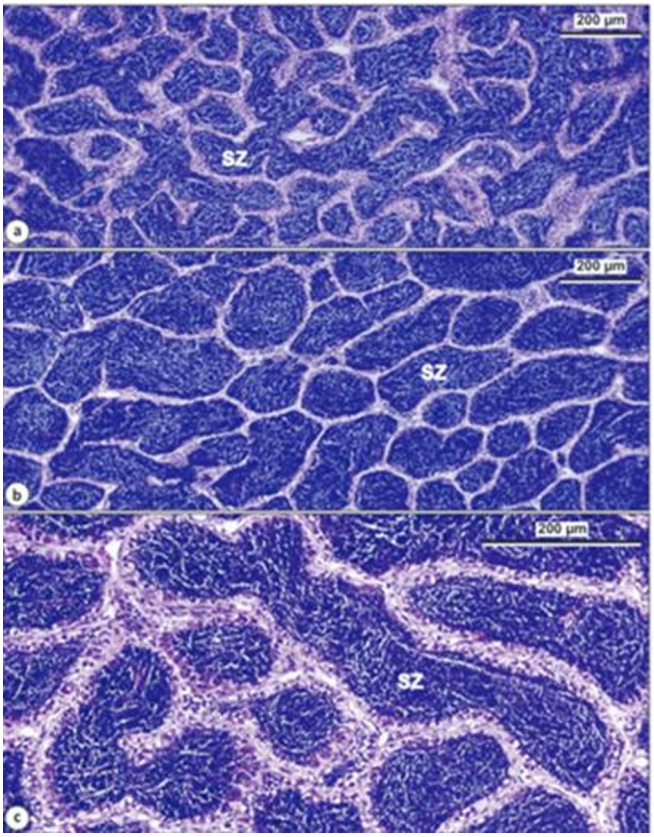


**Fig. 1**. Testes of wild diploid and triploid males of *Carassius gibelio*. On the basis of identical histology documented in the plate, representatives of both diploid (**a**) and triploid males (**b**) included in the study were assigned to the spent reproduction class sensu[45]. (**c**) Seminiferous tubules and germinal epithelium seen in higher magnification. SZ: spermatozoa.

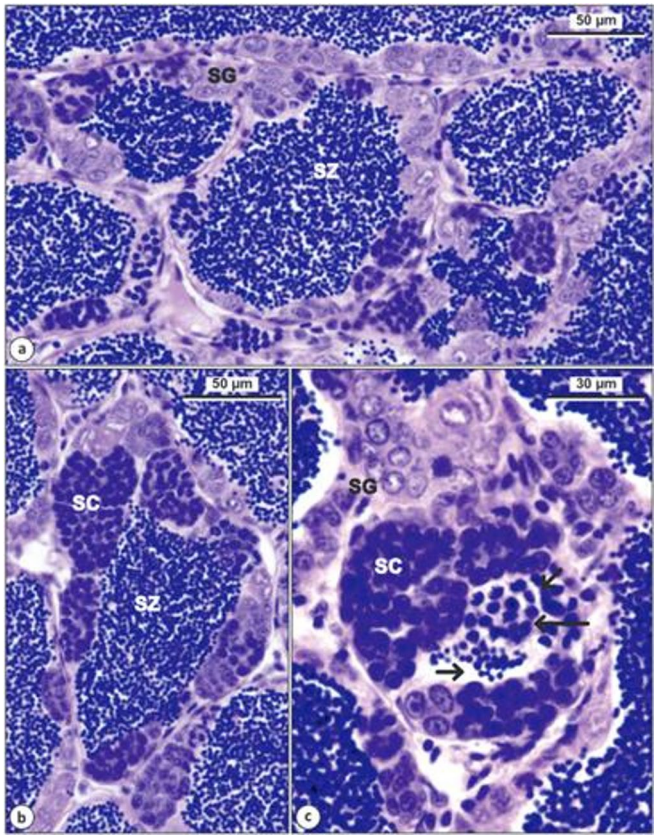


**Fig. 2**. Testes of laboratory-reared genotypic diploid and temperature-induced triploid males of *Carassius gibelio* (**a**-**c**). On the basis of histology, representatives of both diploid and induced triploid males included in the study were assigned to the maturing (early/advanced) reproduction classes sensu Brown-Peterson et al.[45]. Legend: SG: spermatogonia, SC: spermatocytes, arrows highlight spermatids, SZ: spermatozoa.

only at high temperature (male group 1); sex reversal over a wide temperature range with males sampled at high temperature (male group 2); and males sampled at low temperature (male group 3), were not separated from each other by the first two PC axes, and were not separated from each other on the heatmap (Fig. 3). To compare the expression levels of reproduction-related genes between genotypic males and temperature-induced males (including the three groups of induced males), a set of 40 genes related to meiosis[46] (listed in Table 1), and a set of genes involved in male sex determination (listed in Table 2), were selected. PCA based on each of these gene sets showed a partial overlap between temperature-induced and genotypic males along two PC axes, especially for the meiosis-associated gene set (Fig. 4B); however, temperature-induced and genotypic males tended to be separated along PC1 when using male sex-determination genes (Fig. 4C).

## GO enrichment analysis

The DEGs were subsequently annotated to Gene Ontology terms and KEGG pathways. The enriched GO terms are presented in Fig. 5. Several GO terms that were enriched in genotypic males were related to sex differentiation and reproduction. In the biological process category (Fig. 5A), GO terms associated with cell cycle control were enriched in genotypic diploid males, such as DNA recombination (GO:0006310), DNA repair (GO:0006281), DNA damage response (GO:0006974), telomere maintenance (GO:0000723), telomere organization (GO:0032200), and chromosome organization (GO:0051276). GO terms related to meiosis and reproduction were also enriched in genotypic diploid males, including regulation of meiotic nuclear division (GO:0040020), negative regulation of meiotic nuclear division (GO:0045835), regulation of meiotic cell cycle (GO:0051445), negative regulation of meiotic cell cycle (GO:0051447), and negative regulation of reproductive process (GO:2000242). Enriched GO terms related to cell adhesion included cell adhesion (GO:0007155), cell-matrix adhesion (GO:0007160) and cell adhesion mediated by integrin (GO:0033627) (Fig. 5A). In the molecular function category (Fig. 5B), GO terms enriched in genotypic males included helicase activity (GO:0004386) and DNA helicase activity (GO:0003678). In the cellular component category, GO terms enriched in genotypic diploid males included integrin complex (GO:0008305), protein complex involved in cell adhesion (GO:0098636), and plasma membrane (GO:0005886) (Fig. 5C). Several KEGG pathways related to reproduction were significantly enriched, such as cell cycle (caua04110), motor proteins (caua04814), steroid hormone synthesis (caua00140), cell adhesion molecules (caua04514), ECM-receptor interaction (caua04512), and the regulation of actin cytoskeleton (caua04810) (Fig. 5D).

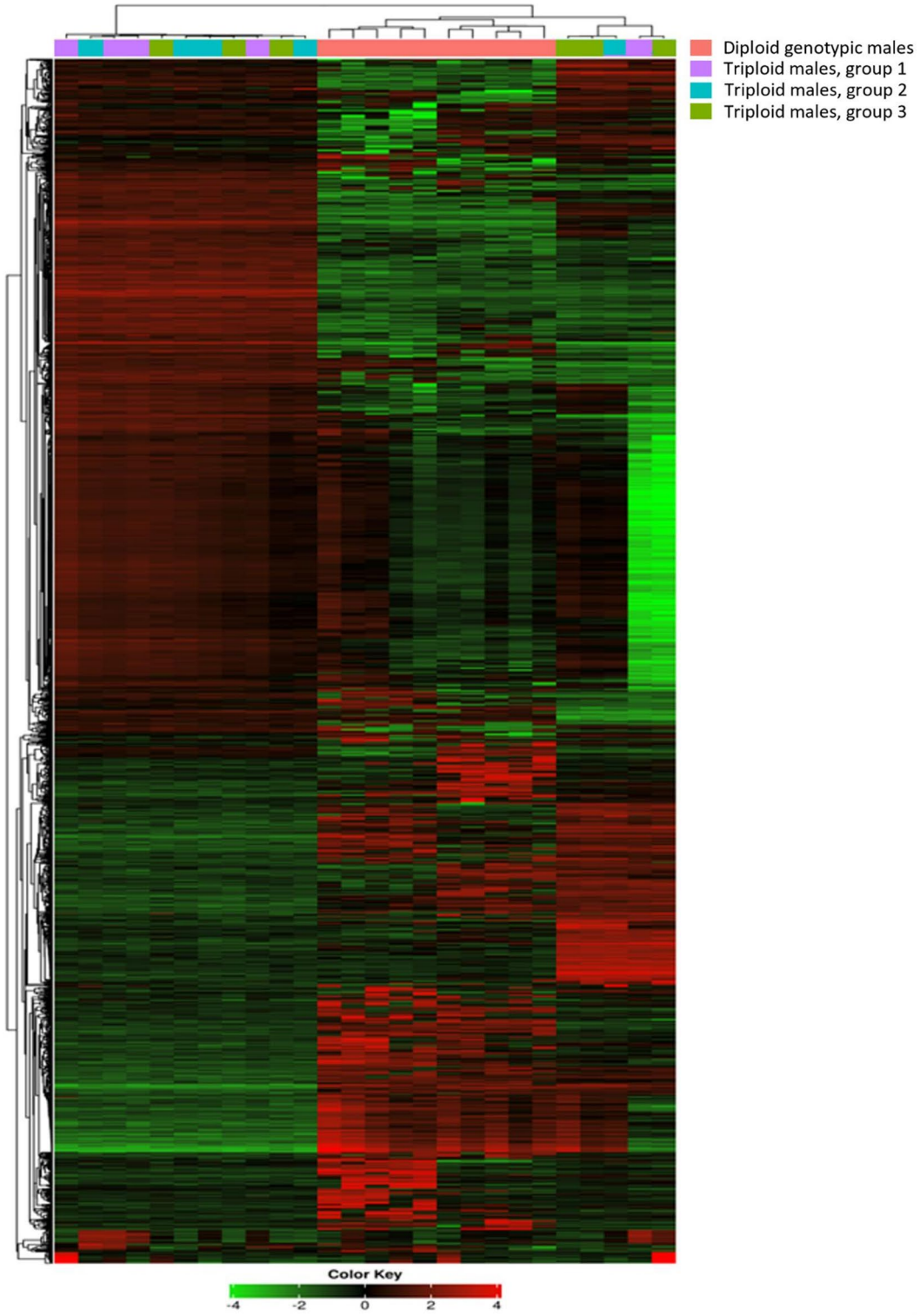


**Fig. 3**. Hierarchical clustering of the relative expression data between genotypic males and temperature-induced males. Diploid genotypic males, and the three groups of temperature-induced triploid males obtained as progeny of gynogenetic females, resulting from sex reversal only at high temperature 28–31 °C (male group 1), sex reversal at 22–31 °C with males sampled at 28–31 °C (male group 2), and males sampled at 22 °C (male group 3), are included. Clustering was based on Pearson's distance and average clustering, based on the top 2000 genes.

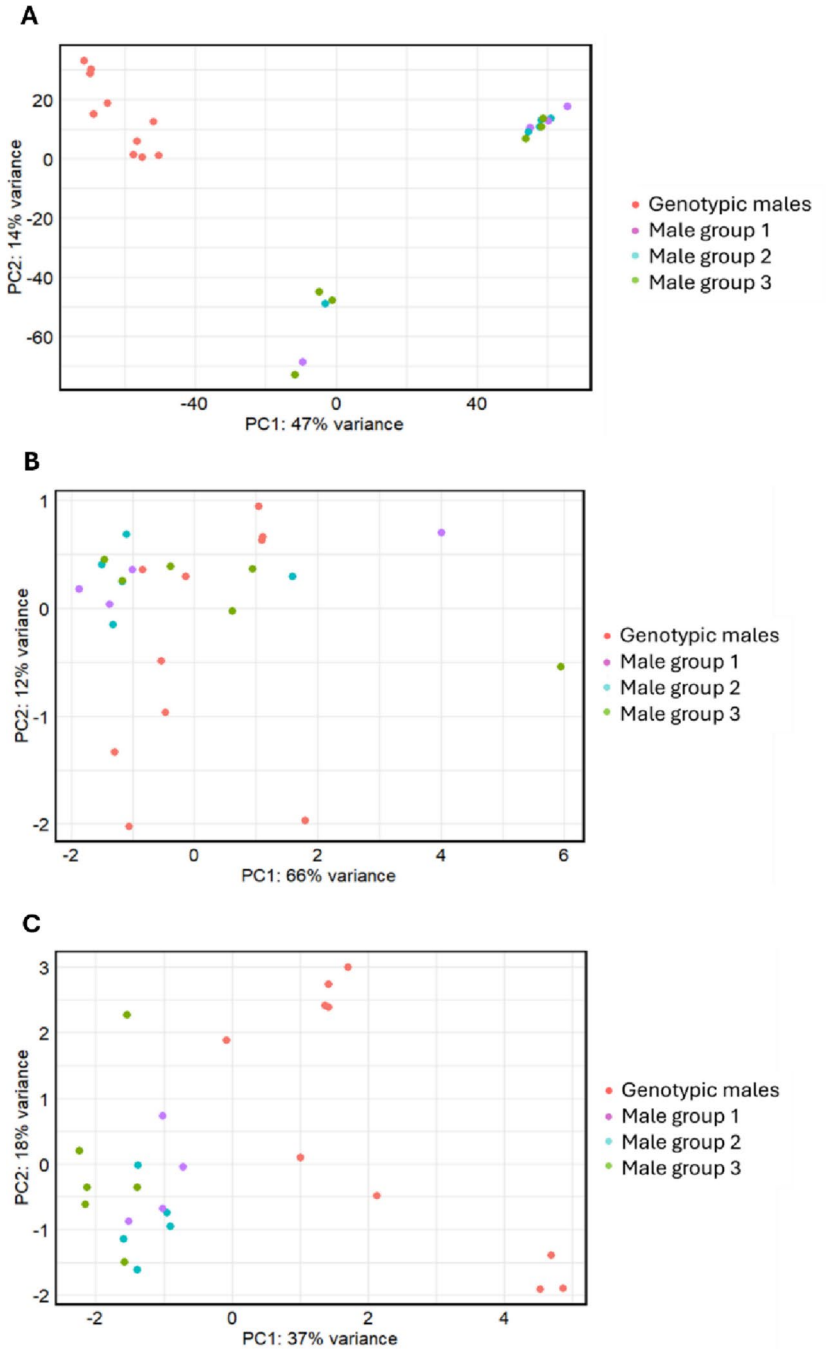


**Fig. 4**. Principal component analysis of normalized RNA-seq read counts between the genotypic and temperature-induced males on the first two principal components. PCA based on all genes (**A**), the meiosis toolkit consisting of 40 genes (**B**), and male sex determination genes (**C**) are presented. The different colours indicate (1) genotypic males (red) and (2) temperature-induced males (i) resulting from sex reversal across the temperature range at 22–31 °C, with males sampled at low temperature (male group 3 - green) and high temperature (male group 2 - blue), or (ii) resulting from sex reversal only at high temperature (male group 1 - purple).

In contrast, several cytoskeleton-associated GO terms were enriched in temperature-induced males (Fig. 5E), such as cytoskeleton (GO:0005856), microtubule-based movement (GO:0007018), microtubule binding (GO:0008017) and microtubule-based process (GO:0007017). In addition, GO terms associated with human pathologies (HP) related to impaired reproduction were also enriched in temperature-induced males and included absent sperm flagella (HP:0032558), infertility (HP:0000789), abnormal sperm tail morphology (HP:0012868), short sperm flagella (HP:0032559), male infertility (HP:0003251), abnormal sperm motility (HP:0012206) and abnormal sperm physiology (HP:0034809).

| Ensembl ID | Gene name | Gene description | L2fc | padj |
|---|---|---|---|---|
| ENSCARG00000016377 | *Spo11* | SPO11 initiator of meiotic double stranded breaks | −0.21 | - |
| ENSCARG00000024429 | *Hormad1* | HORMA domain containing 1 | −0.45 | - |
| **ENSCARG00000034047*** | ***Mnd1*** | **Meiotic nuclear division 1** | **−0.96** | *** |
| **ENSCARG00000050983*** | ***Mlh1*** | **MutL homolog 1** | **0.42** | ** |
| ENSCARG00000069004 | *Mlh3* | MutL homolog 3 | −0.20 | - |
| ENSCARG00000021963 | *Pms1* | PMS homolog 1 | 0.15 | - |
| ENSCARG00000010121 | *Pms2* | PMS homolog 2 | 0.11 | - |
| ENSCARG00000007723 | *Dmc1* | DNA meiotic recombinase 1 | −0.21 | - |
| ENSCARG00000038661 | *Msh2* | MutS homolog 2 | −0.03 | - |
| ENSCARG00000047192 | *Msh4* | MutS homolog 4 | −0.20 | - |
| ENSCARG00000015097 | *Msh5* | MutS homolog 5 | −0.19 | - |
| ENSCARG00000011896 | *Msh6* | MutS homolog 6 | −0.21 | - |
| ENSCARG00000011987 | *Rad1* | Rad1 cohesin complex component | −0.30 | - |
| ENSCARG00000026371 | *Rad21* | Rad21 cohesin complex component | 0.10 | - |
| ENSCARG00000022693 | *Rad50* | Rad50 double strand repair protein | −0.01 | - |
| **ENSCARG00000002053*** | ***Rad51c*** | **Rad51 recombinase** | **−0.54** | * |
| **ENSCARG00000010638*** | ***Rad51b*** | **Rad51 recombinase** | **−0.73** | ** |
| ENSCARG00000018365 | *Rad51d* | RAD51 recombinase | 0.01 | - |
| ENSCARG00000027817 | *Rad51* | RAD51 recombinase | −0.23 | - |
| ENSCARG00000056842 | *Rad51* | RAD51 recombinase | −0.13 | - |
| ENSCARG00000064885 | *Rad51b* | RAD51 recombinase | 0.33 | - |
| ENSCARG00000047813 | *Rad51* | RAD51 recombinase | 0.13 | - |
| ENSCARG00000004144 | *Rad51* | RAD51 recombinase | −0.05 | - |
| **ENSCARG00000045888** | ***Rad52*** | **Rad52 DNA repair protein** | **−0.45** | * |
| ENSCARG00000039864 | *Rec8* | Rec8 meiotic recombination protein | −0.08 | - |
| ENSCARG00000032822 | *Rec114* | Rec114 meiotic recombination protein | −0.08 | - |
| ENSCARG00000057676 | *Smc1b* | Structural maintenance of chromosome 1b | −0.07 | - |
| ENSCARG00000039472 | *Smc1a* | Structural maintenance of chromosome 1a | −0.17 | - |
| ENSCARG00000005430 | *Smc2* | Structural maintenance of chromosome 2 | −0.13 | - |
| ENSCARG00000055515 | *Smc3* | Structural maintenance of chromosome 3 | −0.31 | - |
| **ENSCARG00000010356*** | ***Smc4*** | **Structural maintenance of chromosome 4** | **−0.66** | * |
| ENSCARG00000042929 | *Smc5* | Structural maintenance of chromosome 5 | −0.09 | - |
| ENSCARG00000021147 | *Pds5a* | PDS5 cohesin associated factor B | −0.16 | - |
| ENSCARG00000017951 | *Pds5b* | PDS5 cohesin associated factor B | 0.18 | - |
| ENSCARG00000001906 | *Stag1a* | Cohesin subunit SA 1 A | 0.37 | - |
| ENSCARG00000022475 | *Stag1b* | Cohesin subunit SA 1B | 0.00 | - |
| ENSCARG00000052961 | *Mre11* | Double strand break repair nuclease | 0.21 | - |
| ENSCARG00000018605 | *Hfm1 (Mer3)* | Helicase for meiosis 1 | −0.10 | - |
| ENSCARG00000053878 | *Slc39a1* | Solute carrier family 39A1 | 0.18 | - |
| ENSCARG00000062463 | *Mus81* | Crossover junction endonuclease MUS81 | 0.14 | - |

**Table 1**. List of meiosis genes with their expression levels in genotypic and temperature-induced males. Positive log2 fold change (l2fc) indicates transcripts that were more abundant in genotypic males. Negative log2 fold change indicates transcripts that were more abundant in induced males. Bold indicates significant differences in gene expression level between genotypic and induced males (padj < 0.05). Asterisks indicate significant differences in gene expression level between genotypic and induced males: * padj < 0.05, ** padj < 0.01, *** padj < 0.001, - indicates padj > 0.05.

## Expression of meiosis-associated genes

To determine whether meiosis-associated pathways are disrupted in induced triploid males of *C. gibelio*, we analysed the differences in gene expression levels with respect to an exhaustive list of meiosis-specific genes. Of the set of 40 meiosis-specific genes, all were detected in induced triploid and genotypic diploid males, except *hormad2* (Table 1). Six genes were significantly differentially expressed. *Mlh1 (mutl homologue 1)* displayed slightly higher expression levels in genotypic diploid males, whereas *mnd1 (meiotic nuclear division 1)*, the recombinase encoding genes *rad51b*, *rad51c* and *rad52*, and *smc4* (*structural maintenance of the chromosome 4*) were significantly more highly expressed in induced triploid males. The other meiosis-associated genes, including the meiotic recombination gene *dmc1* and the DNA repair protein-encoding genes *rad21* and several

| Ensembl ID | Gene name | Gene description | L2fc | padj |
|---|---|---|---|---|
| **ENSCARG00000021243** | ***Amh*** | **Anti-Müllerian hormone** | **1.46** | *** |
| **ENSCARG00000000448** | ***Cirbpa*** | **Cold-inducible RNA-binding protein A** | −0.61 | ** |
| **ENSCARG00000069389** | ***Cyp19a1a*** | **Cytochrome P450 19 A1a** | **2.63** | *** |
| ENSCARG00000015111 | *Dmrt1* | Doublesex and mab-3 related transcription factor 1 | 0.09 | |
| ENSCARG00000031029 | *Dmrt1* | Doublesex and mab-3 related transcription factor 1 | 0.15 | |
| ENSCARG00000031374 | *Dmrt2a* | Doublesex and mab-3 related transcription factor 2a | 0.63 | |
| ENSCARG00000015272 | *Dmrt2a* | Doublesex and mab-3 related transcription factor 2a | −0.04 | |
| ENSCARG00000013496 | *Dmrt2b* | Doublesex and mab-3 related transcription factor 2b | 0.21 | |
| **ENSCARG00000028285** | ***Dmrt2b*** | **Doublesex and mab-3 related transcription factor 2b** | **−0.78** | * |
| **ENSCARG00000019977** | ***Dmrta2*** | **Doublesex and mab-3 related transcription factor a2** | **2.05** | * |
| ENSCARG00000003716 | *Foxl2b* | Forkhead box L2 | 0.05 | |
| ENSCARG00000036645 | *Gata4* | GATA-Binding Factor 4 | 0.65 | |
| ENSCARG00000033885 | *Gdf6a* | Growth Differentiation Factor 6 | −0.41 | |
| **ENSCARG00000055889** | ***Gsdf*** | **Gonadal soma-derived factor** | **1.55** | *** |
| ENSCARG00000015482 | *Igf1* | Insulin-like growth factor | −0.89 | |
| **ENSCARG00000058304** | ***Lhx9*** | **LIM Homeobox 9** | **1.83** | *** |
| ENSCARG00000046772 | *Nr0b1 (Dax1)* | Nuclear receptor 0 B1 | 0.05 | |
| ENSCARG00000003021 | *Rspo1* | R-spondin 1 | −0.44 | |
| ENSCARG00000066647 | *Rspo1* | R-spondin 1 | 0.42 | |
| **ENSCARG00000043864** | ***Sf1 (nr5a1a)*** | **steroidogenic factor 1** | **−0.66** | *** |
| **ENSCARG00000052578** | ***Sox4b*** | **SRY-box 4b** | **−1.88** | *** |
| **ENSCARG00000050582** | ***Sox7*** | **SRY-box 7** | **−2.01** | *** |
| **ENSCARG00000058624** | ***Sox8a*** | **SRY-box 8a** | **0.91** | ** |
| **ENSCARG00000033646** | ***Sox9b*** | **SRY-box 9b** | **0.67** | * |
| **ENSCARG00000021129** | ***Star*** | **Steroidogenic acute regulatory protein** | **0.95** | * |
| **ENSCARG00000046195** | ***Wt1a*** | **Wilm's tumor 1a** | **−0.76** | * |

**Table 2**. List of sex determination genes with their differential expression levels between genotypic and temperature-induced males. Positive log2 fold change (l2fc) indicates transcripts that were more abundant in genotypic diploid males. Negative log2 fold change indicates transcripts that were more abundant in temperature-induced triploid males. Bold indicates significant differences in gene expression level between genotypic and induced males (padj < 0.05). Asterisks indicate significant differences in gene expression level between genotypic and induced males (shown in bold): * padj < 0.05, ** padj < 0.01, *** padj < 0.001.

*rad51* homologues, did not show significant differences in gene expression between genotypic and induced males (Table 1).

## Expression of male differentiation genes

To analyse the differences between genotypic and temperature-induced males, we focused on a set of sex-determination genes described in the literature[7,47–51] (Table 2). Genes more highly expressed in genotypic males included *amh* (anti-Müllerian hormone), *sox8a* and *sox9b* (SRY-box transcription factors 8 and 9), *gsdf* (*gonadal soma-derived factor*), and *dmrta2 (dmrt-like family A2)*. Conversely, *sox4b* and *sox7* (SRY-box transcription factors), *cirbpa*, and *dmrt2b* were more highly expressed in induced males, as well as *nr5a1* (*sf1*, steroidogenic factor) and *wt1a* (Wilm's tumor 1a) (Table 2). Other major male-differentiation genes, such as *foxl2b* and *dmrt1*, did not show significant differences in expression between genotypic and temperature-induced males.

## Differentially expressed reproductive genes

Among the 9696 genes that were differentially expressed between genotypic and induced males, we identified 156 genes related to cell cycle control, signalling pathways such as MAPK-dependent signalling, BMP signalling and TGF-β signalling, sex differentiation, steroid synthesis, cytoskeleton, cell motility or involved in spermatogenesis, including sperm flagellum function and sperm-egg interaction (Tables 3, 4 and 5; Fig. 6). Sixteen of these genes were used for confirmation by qRT-PCR (Fig. 7).

## Cell cycle control and meiosis

Several genes involved in cell division and cell cycle control were differentially expressed between genotypic diploid males and temperature-induced triploid males (Table 3, Supplementary Fig. 1). Genes more highly expressed in genotypic males included *adcy1a* (*adenylate cyclase 1a*), *camk2a (Ca/calmodulin kinase IIa*) and *camkk1b* (*Ca/calmodulin-dependent protein kinase kinase 1b*), several *cdkn2c* paralogues encoding the CDK inhibitor p18 (Ink4c), *cdkn1* encoding the protein p27 (Kip1), the early mitotic inhibitor *emi1* (*fbxo5*), *gsk3b* (*glycogen synthase kinase 3β*), and *fgd5* (*fyve, rhogef and ph domain containing protein*) (Supplementary Fig.

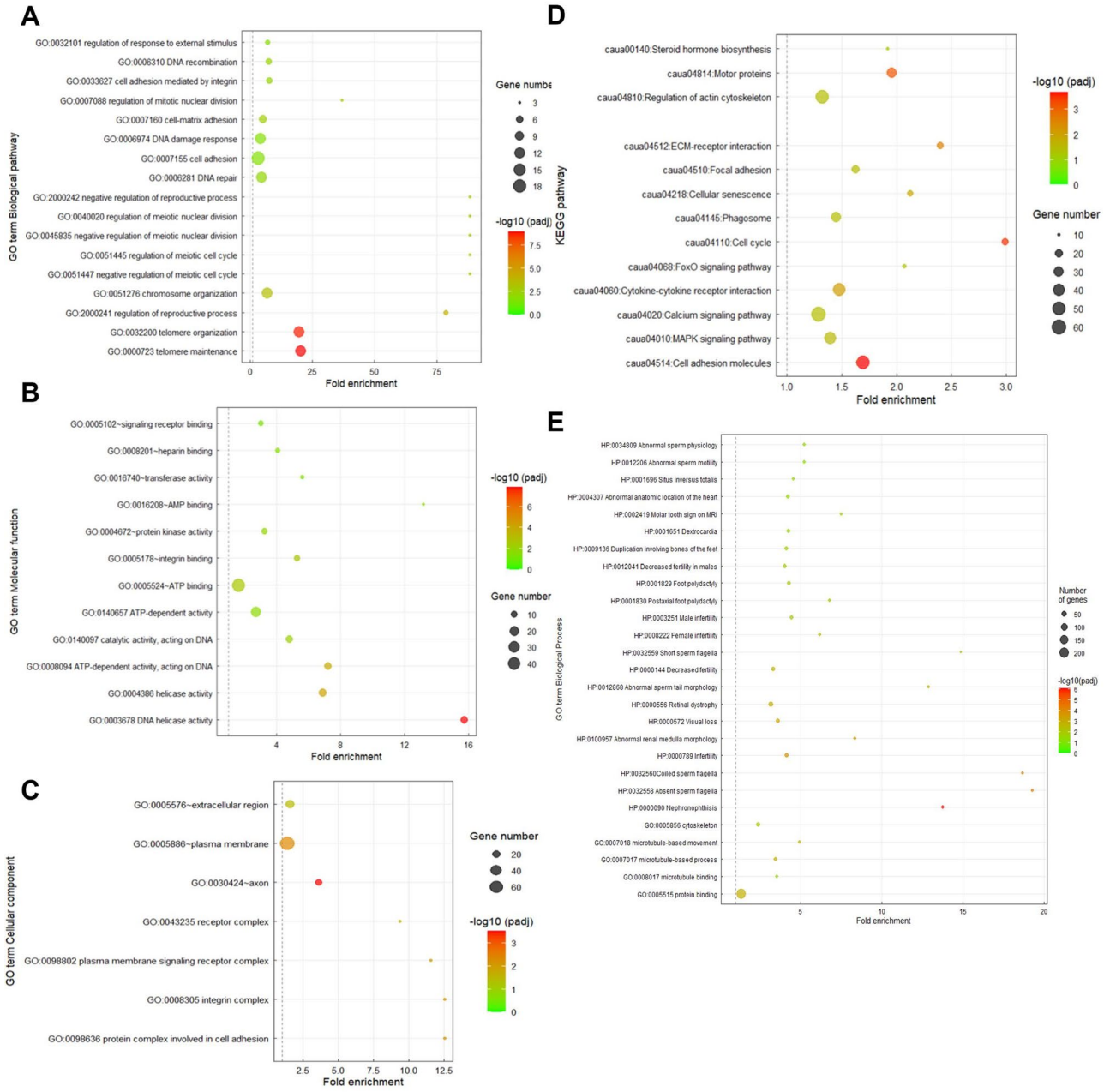


**Fig. 5**. Scatter charts of overrepresented GO terms in genotypic males compared to induced ones. GO term enrichment analysis from the total set of genes that are differently regulated between genotypic males and temperature-induced males in the biological process (**A**), molecular function (**B**) and cellular component (**C**) categories, scatter chart of enriched KEGG pathways in genotypic males compared to temperature-induced males (**D**), and scatter chart of overrepresented GO terms and Human Pathology (HP) terms in temperature-induced males compared to genotypic males (**E**), are presented. The x-axis represents the fold enrichment (the number of DEGs in the GO term/the number of all DEGs)/(the number of genes annotated in this pathway/the number of the genes annotated in all pathways) of each pathway. The y-axis corresponds to the enriched GO terms. The magnitude of dots represents the number of DEGs in the GO term to illustrate pathway size in relation to its enrichment significance, and the color corresponds to the -log10 of the adjusted p-value.

1). By contrast, several genes were more expressed in temperature-induced males, such as *anapc1* and *anapc15* (*apc/c*, encoding the anaphase promoting complex/cyclosome); two *cdc20* paralogues, *mad2l2* (*mitotic arrest deficient 2-like 2*); *bubr1* (encoding a serine/threonine kinase); *ccna* (*cyclin A*) and several *ccnb* paralogues (*cyclin B*); two *e2f1* paralogues, *gadd45aa* and *gadd45ba* (*growth arrest and DNA damage 45*); *fzr1* (*cdh1*, encoding the anaphase promoting complex activator Fizzy-related homolog 1); *cpeb* (*cytoplasmic polyadenylation element binding*), *map2k1* (*mek1*, which encodes the mitogen-activated protein kinase 1); and *ppp2ca* (*pp2a*, which encodes the protein phosphatase 2) (Supplementary Fig. 1).

| Ensembl ID | Gene name | Gene description in Ensembl | Function | L2fc | padj |
|---|---|---|---|---|---|
| ENSCARG00000015415 | *Adcy1a* | Adenylate Cyclase Type 1-Like | cAMP formation | 3.41 | *** |
| ENSCARG00000017301 | *Anapc1* | Anaphase Promoting Complex Subunit 1 | Cell cycle control and mitosis | −0.53 | * |
| ENSCARG00000005820 | *Anapc15* | Anaphase Promoting Complex Subunit 15 | Cell cycle control and mitosis | −0.93 | *** |
| ENSCARG00000008486 | *Bubr1* | Serine/Threonine-Protein Kinase BUB1 β-Like | Spindle checkpoint | −0.91 | ** |
| ENSCARG00000023912 | *Camk2a* | Ca-Dependent Protein Kinase Kinase 1-Like | Calmodulin-dependent protein kinase complex | 1.94 | *** |
| ENSCARG00000015494 | *Camkk1b* | Ca-Dependent Protein Kinase Kinase 1-Like | Calmodulin-dependent protein kinase complex | 2.56 | *** |
| ENSCARG00000067900 | *Camk1ga* | Ca-dependent Protein Kinase Type 1D-Like | Calmodulin-dependent protein kinase complex | −0.80 | *** |
| ENSCARG00000006057 | *Camk1ga* | Ca-Dependent Protein Kinase Type 1D-Like | Calmodulin-dependent protein kinase complex | 0.98 | *** |
| ENSCARG00000066013 | *Ccnb2* | G2/Mitotic-Specific Cyclin-B2-Like | Cell cycle control | −0.99 | *** |
| ENSCARG00000062532 | *Ccnb3* | G2/Mitotic-Specific Cyclin-B3-Like | Cell cycle control | −1.03 | *** |
| ENSCARG00000007196 | *Ccnb3* | G2/Mitotic-Specific Cyclin-B3-Like | Cell cycle control | −0.51 | * |
| ENSCARG00000054013 | *Csnk1db* | Casein Kinase 1, Delta B | Mitotic spindle | 0.64 | *** |
| ENSCARG00000016635 | *Csnk1g1* | Casein Kinase I | Cell division | −2.80 | *** |
| ENSCARG00000027165 | *Cdc20* | Cell Division Cycle Protein 20 Homolog | Cell cycle control | −1.78 | *** |
| ENSCARG00000005591 | *Cdc20* | Cell Division Cycle Protein 20 Homolog | Cell cycle control | −1.28 | *** |
| ENSCARG00000069709 | *Cenpn* | Centromere Protein N-Like | Chromosome organization | −1.14 | *** |
| ENSCARG00000022613 | *Ccnb1* | Cyclin B1 | Cell cycle control | −1.09 | *** |
| ENSCARG00000034712 | *Ccnb2* | Cyclin B2 | Cell cycle control | −0.70 | ** |
| ENSCARG00000044731 | *Ccna2* | Cyclin-A2-Like | Cell cycle control | −2.31 | *** |
| ENSCARG00000028136 | *Ccnb1* | G2/Mitotic-Specific Cyclin-B1 | Cell cycle control | −1.19 | *** |
| ENSCARG00000030662 | *Cdc25b* | M-Phase Inducer Phosphatase 1-Like | Cell cycle control | −1.01 | *** |
| ENSCARG00000023741 | *Cdc25b* | M-Phase Inducer Phosphatase 1-Like | Cell cycle control | −1.06 | *** |
| ENSCARG00000068799 | *Cdkn2c* | Cyclin-Dependent Kinase 4 Inhibitor C-Like | Cell cycle control | 1.79 | *** |
| ENSCARG00000062841 | *Cdkn2c* | Cyclin-Dependent Kinase 4 Inhibitor C-Like | Cell cycle control | 1.70 | *** |
| ENSCARG00000005953 | *Cdkn1ba* | Cyclin-Dependent Kinase Inhibitor 1B-Like | Cell cycle control | 0.97 | *** |
| ENSCARG00000026445 | *Cdkn1ba* | Cyclin-Dependent Kinase Inhibitor 1B-Like | Cell cycle control | 0.67 | ** |
| ENSCARG00000013903 | *Cdkn1ca* | Cyclin-Dependent Kinase Inhibitor 1 C-Like | Cell cycle control | 0.45 | * |
| ENSCARG00000055647 | *Cdkn1a* | Cyclin-Dependent Kinase Inhibitor 1-Like | Cell cycle control | 0.47 | * |
| ENSCARG00000060407 | *Ccn f* | Cyclin-F-Like | Cell cycle control | −1.76 | *** |
| ENSCARG00000013683 | *Cpeb1a* | Cytoplasmic Polyadenylation Element Binding Protein 1a | Cell cycle control | −0.85 | *** |
| ENSCARG00000058210 | *Ddx2* | Probable ATP-Dependent RNA Helicase DDX2 | RNA helicase | −0.58 | *** |
| ENSCARG00000010183 | *Ddx52* | DEAD (Asp-Glu-Ala-Asp) Box Polypeptide 52 | Ribosome biogenesis, cell cycle control | 1.37 | *** |
| ENSCARG00000006396 | *E2f1* | E2F Transcription Factor 1 | Cell cycle control | −1.12 | *** |
| ENSCARG00000009185 | *E2f1* | E2F Transcription Factor 1 | Cell cycle control | −2.37 | *** |
| ENSCARG00000056526 | *Emi1 (fbxo5)* | F-Box Only Protein 5-Like | Cell cycle control | 2.89 | *** |
| ENSCARG00000013439 | *Emi1 (fbxo5)* | F-Box Only Protein 5-Like | Cell cycle control | 1.38 | *** |
| ENSCARG00000037330 | *Fbxo15* | F-Box Protein 15 | Cell cycle control | −1.03 | ** |
| ENSCARG00000018093 | *Emi1 (fbxo5)* | F-Box Protein 5 | Cell cycle control | 1.20 | *** |
| ENSCARG00000055566 | *Fgd5* | FYVE, RhoGEF and PH Domain Containing 5 | Cell cycle control | 0.91 | ** |
| ENSCARG00000038535 | *Fzr1a (cdh1)* | Fizzy/Cell Division Cycle 20 Related 1a | Anaphase promoting complex activity | −0.85 | *** |
| ENSCARG00000081132 | *Gsk3b* | Glycogen Synthase Kinase 3 Beta | Cell cycle control, meiosis | 1.01 | ** |
| ENSCARG00000004515 | *Gadd45aa* | Growth Arrest and DNA Damage-Inducible Protein | Cell cycle control | −1.19 | *** |
| ENSCARG00000056928 | *Gadd45ba* | Growth Arrest and DNA Damage-Inducible Protein | Cell cycle control | −1.14 | *** |
| ENSCARG00000062672 | *Mad2l2* | Mitotic Arrest Deficient 2-like 2 | Cell cycle control | −1.03 | ** |
| ENSCARG00000001430 | *Map2k1* | Dual Specificity Mitogen-Activated Protein Kinase Kinase 1 L | MAPK signalling pathway | −1.16 | *** |
| ENSCARG00000023751 | *Mnd1* | Meiotic Nuclear Divisions 1 Homolog | Meiosis | −0.96 | *** |
| ENSCARG00000058155 | *Ppp2ca* | Protein Phosphatase 2, Catalytic Subunit, α Isozyme | Cell growth and cell cycle control | −0.80 | *** |
| ENSCARG00000045179 | *Rfc4* | Replication Factor C Subunit 4-Like | DNA replication | 0.59 | *** |
| ENSCARG00000000918 | *Spinb* | Spindlin-Z-Like | Cell division and meiosis | −0.79 | *** |

**Table 3**. List of differentially expressed cell cycle control and meiosis-associated genes between temperature-induced males and genotypic males. The gene function follows the biological databases Uniprot, KEGG, Zfin and GeneCards. Positive log2 fold change (l2fc) indicates transcripts that were more abundant in genotypic males. Negative log2 fold change indicates transcripts that were more abundant in temperature-induced triploid males. Asterisks indicate significant differences in gene expression level between genotypic and induced males: * for padj < 0.05, ** for padj < 0.01, *** for padj < 0.001.

| Ensembl ID | Gene name | Gene description in Ensembl | Function | L2fc | padj |
|---|---|---|---|---|---|
| ENSCARG00000063488 | *Actr10* | Actin Related Protein 10 | Activates dynein | −0.44 | * |
| ENSCARG00000057794 | *Actr3b* | Actin Related Protein 3B | Regulation of actin polymerization | 1.60 | *** |
| ENSCARG00000044296 | *Arpc1b* | Actin-Related Protein 2/3 Complex Subunit 1B-Like | Actin polymerization | −1.47 | *** |
| ENSCARG00000012523 | *Actr2b* | Actin-Related Protein 2-B-Like | Mediates actin polymerization | −0.60 | *** |
| ENSCARG00000054971 | *Apc2* | Adenomatous Polyposis Coli Protein 2-Like | Stabilization of the cytoskeleton | 1.05 | ** |
| ENSCARG00000020833 | *Baiap2l2a* | brain-specific angiogenesis inhibitor 1-associated protein 2-l2a | Cytoskeleton organization | 1.02 | *** |
| ENSCARG00000005444 | *Cd9a* | Tetraspanin 29 | Sperm-egg adhesion | −1.15 | *** |
| ENSCARG00000005444 | *Cd9b* | Tetraspanin 29 | Sperm-egg adhesion | 1.01 | ** |
| ENSCARG00000041240 | *Cfl1* | Cofilin 1 | Cell division and cytoskeleton | −0.45 | ** |
| ENSCARG00000048314 | *Cfl1l* | Cofilin 1 (Non-Muscle), Like | Cell division and cytoskeleton | 0.39 | * |
| ENSCARG00000055139 | *Cfl2* | Cofilin 2 (Muscle) | Cell division and cytoskeleton | 1.27 | *** |
| ENSCARG00000062621 | *Cfl1l* | Cofilin-2-Like | Cell division and cytoskeleton | 0.65 | * |
| ENSCARG00000012813 | *Diaph3* | Diaphanous-Related Formin 3 | Cytoskeleton organization | −1.36 | *** |
| ENSCARG00000033789 | *Dnahc17* | Dynein Axonemal Heavy Chain 17 | Molecular motor | −1.03 | * |
| ENSCARG00000016098 | *Dnai2b* | Dynein Intermediate Chain 3, Ciliary-Like | Molecular motor | 1.10 | *** |
| ENSCARG00000015806 | *Dnai3* | WD repeat domain 63 | Cell migration | −0.99 | * |
| ENSCARG00000020846 | *Dnal4a* | Dynein Light Chain 1, Axonemal-Like | Molecular motor | −0.83 | * |
| ENSCARG00000067868 | *Dnal1* | Dynein Light Chain 4, Axonemal | Molecular motor | −1.54 | * |
| ENSCARG00000066325 | *Dnah5* | Dynein, Axonemal, Heavy Chain 5 | Molecular motor | −0.88 | * |
| ENSCARG00000015354 | *Dync1i1* | Dynein, Cytoplasmic 1, Intermediate Chain 1 | Molecular motor | −0.66 | *** |
| ENSCARG00000041117 | *Fgf14* | Fibroblast Growth Factor 14 | Mitogenic activities | −0.98 | *** |
| ENSCARG00000033052 | *Fgf14* | Fibroblast Growth Factor 14 | Mitogenic activities | −0.95 | ** |
| ENSCARG00000002073 | *Fgf24* | Fibroblast Growth Factor 18-Like | Mitogenic activities | 1.65 | *** |
| ENSCARG00000068748 | *Fgf4* | Fibroblast Growth Factor 4 | Mitogenic activities | 1.11 | * |
| ENSCARG00000010217 | *Fgf8a* | Fibroblast Growth Factor 8-Like | Mitogenic activities | 0.71 | *** |
| ENSCARG00000031169 | *Fn1b* | Fibronectin-Like | Cell adhesion and migration | 2.16 | *** |
| ENSCARG00000054160 | *Gsna* | Gelsolin a | Cytoskeleton assembly | −0.69 | ** |
| ENSCARG00000045339 | *Lpar2a* | lysophosphatidic acid receptor 2a | Cytoskeleton organization | 0.44 | ** |
| ENSCARG00000045339 | *Lpar5* | lysophosphatidic acid receptor 5 | Cytoskeleton organization | −0.87 | * |
| ENSCARG00000028260 | *Itga2* | Integrin Alpha-2-Like | Cell adhesion | 1.59 | ** |
| ENSCARG00000058212 | *Itga11a* | Integrin Alpha-11 | Cell adhesion | −1.59 | *** |
| ENSCARG00000023759 | *Itga4* | Integrin Alpha-4 | Cell adhesion | 1.64 | *** |
| ENSCARG00000056600 | *Itga6* | Integrin Alpha-6 | Cell adhesion | 1.46 | *** |
| ENSCARG00000000507 | *Itga6b* | Integrin Alpha-6b | Cell adhesion | 1.34 | *** |
| ENSCARG00000019599 | *Itga8* | Integrin Alpha-8 | Cell adhesion | 1.57 | *** |
| ENSCARG00000053400 | *Itga8* | Integrin Alpha-8 | Cell adhesion | −1.06 | *** |
| ENSCARG00000052085 | *Itgm* | Integrin Alpha-M | Cell adhesion | −1.17 | *** |
| ENSCARG00000044418 | *Itga10* | Integrin Alpha-10 | Cell adhesion | −1.64 | ** |
| ENSCARG00000049815 | *Izumo* | Izumo Sperm-Specific Protein | Sperm-egg recognition | 2.74 | * |
| ENSCARG00000049229 | *Kif23* | Kinesin Family Member 23 | Molecular motor | −0.89 | ** |
| ENSCARG00000057752 | *Kif26aa* | Kinesin Family Member 26Aa | Molecular motor | −1.99 | *** |
| ENSCARG00000043633 | *Kif26aa* | Kinesin Family Member 26Aa | Molecular motor | −3.29 | *** |
| ENSCARG00000032249 | *Kif26ab* | Kinesin Family Member 26Ab | Molecular motor | −1.42 | *** |
| ENSCARG00000010175 | *Klc3* | Kinesin Light Chain 3 | Molecular motor | 0.70 | *** |
| ENSCARG00000012280 | *Kif1ab* | Kinesin-1 Heavy Chain-Like | Molecular motor | 1.07 | * |
| ENSCARG00000025626 | *Kif11* | Kinesin-Like Protein KIF11 | Molecular motor | −0.77 | * |
| ENSCARG00000024504 | *Kif16ba* | Kinesin-Like Protein KIF16B | Molecular motor | 0.31 | * |
| ENSCARG00000067451 | *Kif1ab* | Kinesin-Like Protein KIF1A | Molecular motor | 1.03 | * |
| ENSCARG00000008396 | *Kif5ba* | Kinesin-Like Protein KIF1A | Molecular motor | −1.01 | *** |
| ENSCARG00000055954 | *Kif21a* | Kinesin-Like Protein KIF21A | Molecular motor | 0.62 | *** |
| ENSCARG00000043633 | *Kif26aa* | Kinesin-Like Protein KIF26A | Molecular motor | −3.29 | *** |
| ENSCARG00000064202 | *M1ap* | Meiosis 1 Associated Protein | Spermatogenesis | 0.58 | * |
| ENSCARG00000053540 | *Myo1b* | Myosin 1b | Cell motility | 1.05 | ** |
| ENSCARG00000065661 | *Myo3a* | Myosin 3a | Cell motility | 1.36 | ** |
| ENSCARG00000022649 | *Myo3b* | Myosin 3b | Cell motility | −1.61 | *** |
| ENSCARG00000058703 | *Myo5aa* | Myosin 5aa | Cell motility | −1.25 | *** |

Continued

| Ensembl ID | Gene name | Gene description in Ensembl | Function | L2fc | padj |
|---|---|---|---|---|---|
| ENSCARG00000025821 | *Myo7ab* | Myosin 7ab | Molecular motor | −1.47 | *** |
| ENSCARG00000014750 | *Myo10l1* | Myosin 10, Like 1 | Molecular motor | 1.37 | *** |
| ENSCARG00000069662 | *Myo15b* | Myosin 15 | Molecular motor | 1.42 | *** |
| ENSCARG00000056359 | *Pak1* | P21 (RAC1) Activated Kinase 1 | Cytoskeleton organization | −0.57 | * |
| ENSCARG00000008473 | *Pak6a* | P21 Activated Kinase 6a | Cytoskeleton organization, Androgen signalling | −1.14 | *** |
| ENSCARG00000042990 | *Pak7* | P21 (RAC1) Activated Kinase 7 | Cytoskeleton organization | −0.99 | ** |
| ENSCARG00000045144 | *Pfn1* | Profilin 1 | Cytoskeleton organization | −1.40 | * |
| ENSCARG00000004805 | *Piwil2* | Piwi-Like Protein 2 | Spermatocytes differentiation | 0.47 | ** |
| ENSCARG00000044904 | *Plxnb1a* | Plexin-B1-Like | Cell adhesion | −0.46 | * |
| ENSCARG00000019805 | *Rhoab* | Rho-Related GTP-Binding Protein Rhoa-B | Cytoskeleton organization | −1.05 | *** |
| ENSCARG00000007149 | *Spag1a* | Sperm Associated Antigen 1a | Axoneme assembly | 1.29 | *** |
| ENSCARG00000022120 | *Syce2* | Synaptonemal Complex Central Element Protein 2 | Synaptonemal complex assembly | −0.81 | * |
| ENSCARG00000055357 | *Spef2* | Sperm flagellar 2 | Sperm flagellum assembly | 0.92 | * |
| ENSCARG00000056199 | *Tekt4* | Tektin 4 | Spermatogenesis | −1.12 | * |
| ENSCARG00000062861 | *Tekt1* | Tektin-1-Like | Spermatogenesis | −2.09 | *** |
| ENSCARG00000025844 | *Thbs1* | Thrombospondin 1 | Cell adhesion | 1.07 | ** |
| ENSCARG00000051875 | *Thbs2* | Thrombospondin 2 | Cell adhesion | 0.93 | ** |
| ENSCARG00000029783 | *Thbs3* | Thrombospondin 3 | Cell adhesion | 1.50 | *** |
| ENSCARG00000018165 | *Thbs4* | Thrombospondin 4 | Cell adhesion | −1.71 | *** |
| ENSCARG00000002324 | *Tmem67* | Transmembrane Protein 67 | Ciliogenesis | −1.01 | *** |
| ENSCARG00000068821 | *Tnnc2* | Troponin C, Skeletal Muscle | Molecular motor | 2.06 | *** |
| ENSCARG00000050269 | *Tnnc1b* | Troponin C, Slow Skeletal and Cardiac Muscles-Like | Molecular motor | 1.94 | *** |
| ENSCARG00000063547 | *Tnnt3b* | Troponin T Type 3b (Skeletal, Fast) | Molecular motor | 2.05 | * |
| ENSCARG00000034258 | *Tnnt2d* | Troponin T2d, Cardiac | Molecular motor | 1.25 | *** |
| ENSCARG00000062526 | *Wdr19* | WD Repeat Domain 19 | Sperm flagellum | −1.11 | *** |
| ENSCARG00000067233 | *Wdr19* | WD Repeat Domain 19 | Sperm flagellum | −1.37 | *** |

**Table 4**. List of differentially expressed genes associated with spermatogenesis, cytoskeleton and cell motility between genotypic and temperature-induced males males. The gene function follows the biological databases Uniprot, KEGG, Zfin and GeneCards. Positive log2 fold change (l2fc) indicates transcripts that were more abundant in genotypic males. Negative log2 fold change indicates transcripts that were more abundant in temperature-induced triploid males. Asterisks indicate significant differences in gene expression level between genotypic and temperature-induced males: * for padj < 0.05, ** for padj < 0.01, *** for padj < 0.001.

## Spermatogenesis and fertilization

Several genes involved in spermatogenesis and fertilization were differentially expressed between genotypic and temperature-induced males (Table 4). Most importantly, genotypic males strongly overexpressed the crucial fertilization-specific *izumo*, involved in sperm binding to the zona pellucida of the egg, as well as *piwil2* (involved in germ cell maintenance and spermatocyte differentiation). Conversely, a few spermatogenesis and male differentiation genes were more highly expressed in induced males, such as *tekt1* and *tekt4* (encoding tektins, structural components of sperm flagellum). Several genes involved in flagellum structure and motility were also differentially expressed, such as *spef2* (*sperm flagellar 2)* and *spag1a (sperm associated antigen 1a)*, more highly expressed in genotypic males, while *wdr19 (wd repeat domain 19)* was more highly expressed in induced males (Table 4).

## Cytoskeleton and molecular motors

Genes encoding components of the cytoskeleton were differentially expressed between genotypic males and temperature-induced males (Table 4, Supplementary Fig. 2). Genotypic males showed higher expression of constituents of the extracellular matrix and genes involved in cell-cell interactions, including members of the fibroblast growth factor family (*fgf4*, *fgf8a* and *fgf24)*, *lpar2a* (*lysophosphatidic acid receptor 2a*), *fn1b* (*fibronectin 1*); integrins such as *itga2*, *itga4*, *itga6*, *itga6b* and one copy of *itga8*; *baiap2*/*irsp53* (encoding a scaffold involved in cytoskeleton organization); *apc2* (*adenomatous polyposis coli*), and the cofilin family members *cfl1l* and *cfl2* (Supplementary Fig. 2). In contrast, induced males showed higher expression of *rhoab* (*Rho GTPase*); *pak1*, *pak6* and *pak7* (encoding serine/threonine kinases), *pfn1* (*profilin* 1); *arpc1b* (encoding a component of the actin-related protein 2/3 complex), *diaph3* (encoding the diaphanous-related formin 3), integrins *itga8*, *itga10*, *itga11* and *itgm*; *lpar5* (*lysophosphatidic acid receptor 5*), *fgf14* (*fibroblast growth factor 14*), *cfl1* and *gsna* (*gelsolin a*) (Supplementary Fig. 2). Genes encoding molecular motors were differentially expressed between genotypic and induced males (Table 4, Supplementary Fig. 3). Genotypic males showed higher expression of myosin superfamily members, such as *myo1b*, *myo3a*, *myo10l1* and *myo15b* and kinesin family members *kif1ab*, *kif16ba*, *kif21a*, and kinesin light chain (*klc3).* In contrast, induced males showed higher expression of members of the

| Ensembl ID | Gene name | Gene description in Ensembl | Function | L2fc | padj |
|---|---|---|---|---|---|
| ENSCARG00000061469 | *Acvr2ba* | Activin Receptor Type-1-Like | Receptor for the TGF-βeta ligands | −1.32 | *** |
| ENSCARG00000068015 | *Acvr1l* | Activin Receptor Type-1-Like | Receptor for the TGF-βeta ligands | −1.03 | *** |
| ENSCARG00000013161 | *Acvrl1* | Activin Receptor Type-2B-Like | Receptor for the TGF-βeta ligands | 0.97 | *** |
| ENSCARG00000021243 | *Amh* | Anti-Mullerian Hormone | Male fetal sexual differentiation | 1.46 | *** |
| ENSCARG00000012651 | *Bambia* | BMP And Activin Membrane-Bound Inhibitor Homolog | Regulation of TGF-βeta signalling | −0.71 | ** |
| ENSCARG00000067218 | *Bmp2* | Bone morphogenic protein 2 | TGF beta signalling pathway, growth factor | 1.42 | ** |
| ENSCARG00000032554 | *Bmp5* | Bone morphogenic protein 5 | TGF beta signalling pathway, growth factor | 2.09 | *** |
| ENSCARG00000052667 | *Bmp7* | Bone morphogenic protein 7 | TGF beta signalling pathway, growth factor | 1.65 | *** |
| ENSCARG00000030315 | *Bmp8* | Bone morphogenic protein 8 | TGF beta signalling pathway, growth factor | −1.68 | *** |
| ENSCARG00000041569 | *Bmp10* | Bone morphogenic protein 2 | TGF beta signalling pathway, growth factor | 1.60 | ** |
| ENSCARG00000067031 | *Chst6* | Carbohydrate sulfotransferase 6 | Steroid biosynthesis | −1.19 | ** |
| ENSCARG00000050828 | *Comta* | catechol O-methyltransferas | Steroid biosythesis | 1.46 | ** |
| ENSCARG00000070082 | *Cyp17a2* | Cytochrome P450 17 A1a | Steroid biosythesis | 1.60 | ** |
| ENSCARG00000069389 | *Cyp19a1a* | Cytochrome P450 19 A1a | Conversion of androgenes into estrogens | 2.63 | *** |
| ENSCARG00000014711 | *Cyp7a1* | Cytochrome P450 7a1 | Steroid biosythesis | 1.34 | *** |
| ENSCARG00000041117 | *Fgf14* | Fibroblast Growth Factor 14 | Mitogenic activities | −0.98 | *** |
| ENSCARG00000033052 | *Fgf14* | Fibroblast Growth Factor 14 | Mitogenic activities | −0.95 | ** |
| ENSCARG00000002073 | *Fgf24* | Fibroblast Growth Factor 18-Like | Mitogenic activities | 1.65 | *** |
| ENSCARG00000068748 | *Fgf4* | Fibroblast Growth Factor 4 | Mitogenic activities | 1.11 | * |
| ENSCARG00000010217 | *Fgf8a* | Fibroblast Growth Factor 8-Like | Mitogenic activities | 0.71 | *** |
| ENSCARG00000042302 | *Fsta* | Follistatin-A-Like | Gonad differentiation | 0.96 | *** |
| ENSCARG00000049613 | *Fstl1a* | Follistatin-Like 1a | Gonad differentiation | −0.80 | *** |
| ENSCARG00000054976 | *Fstl5* | Follistatin-Like 5 | Gonad differentiation | −1.12 | * |
| ENSCARG00000027726 | *Grapb* | GRB2-Related Adapter Protein-Lik | Ras signalling pathway | 1.65 | ** |
| ENSCARG00000055889 | *Gsdf* | Gonadal soma-derived factor | Gonadal differentiation | 1.55 | *** |
| ENSCARG00000070063 | *Hrasb* | Hras GTPase b | Cell cycle control | −0.49 | * |
| ENSCARG00000014711 | *Hsd17b2* | Hydroxysteroid 17b deshydrogenase 2 | Steroid regulation | −2.48 | *** |
| ENSCARG00000001430 | *Map2k1* | Dual Specificity Mitogen-Activated Protein Kinase Kinase 1 L | MAPK signalling pathway | −1.16 | *** |
| ENSCARG00000020520 | *Ltbp1* | Latent transforming growth factor β binding protein 1 | TGF-β signalling | −0,85 | *** |
| ENSCARG00000039542 | *Rasal3* | Ras protein activator like 3 | Cell cycle control | −0.79 | * |
| ENSCARG00000005085 | *Rasal1b* | Ras protein activator like 1b | Cell cycle control | 1.01 | *** |
| ENSCARG00000025477 | *Rasa3* | Ras protein activator 3 | Cell cycle control | 0.29 | * |
| ENSCARG00000014802 | *Rassf7b* | Ras Association Domain-Containing Protein 7-Like | Cell cycle control | −0.86 | ** |
| ENSCARG00000066514 | *Rps6ka2* | Ribosomal Protein S6 Kinase Alpha-2-Like | MAPK signalling pathway | −1.19 | *** |
| ENSCARG00000065916 | *Rbpms2a* | RNA-Binding Protein with Multiple Splicing 2 | Gonad differentiation | −0.65 | ** |
| ENSCARG00000013605 | *Rbpms2b* | RNA-Binding Protein with Multiple Splicing 2 | Gonad differentiation | −0.79 | *** |
| ENSCARG00000040486 | *Skilb* | Ski-Like Protein | Cell growth and differentiation | 0.55 | ** |
| ENSCARG00000069284 | *Skilb* | Ski-Like Protein | Cell growth and differentiation | 0.45 | ** |
| ENSCARG00000035926 | *Smad3a* | SMAD Family Member 3a | Cell growth and differentiation | 0.65 | *** |
| ENSCARG00000040718 | *Smad4a* | SMAD Family Member 4a | Cell growth and differentiation | −0.36 | ** |
| ENSCARG00000040507 | *Smad7* | SMAD Family Member 7 | Cell growth and differentiation | 0.36 | * |
| ENSCARG00000024144 | *Sox4* | SRY-Box Transcription Factor 4 | Cell differentiation | −0.61 | *** |
| ENSCARG00000050387 | *Sox4* | SRY-Box Transcription Factor 4 | Cell differentiation | −0.80 | * |
| ENSCARG00000052578 | *Sox4b* | SRY-Box Transcription Factor 4b | Cell differentiation | −1.88 | *** |
| ENSCARG0000002614 | *Srd5a2* | Steroid dehydrogenase 2 | Steroid biosythesis | 1.76 | ** |
| ENSCARG00000070139 | *Sox14* | Transcription Factor Sox-14-Like | Cell differentiation | 1.46 | * |
| ENSCARG00000014763 | *Sox2* | Transcription Factor Sox-2 | Cell differentiation | 0.93 | *** |
| ENSCARG00000050335 | *Sox4b* | Transcription Factor SOX-4-Like | Cell differentiation | −1.51 | *** |
| ENSCARG00000053331 | *Sox4b* | Transcription Factor SOX-4-Like | Cell differentiation | −1.74 | * |
| ENSCARG00000050582 | *Sox7* | Transcription Factor Sox-7-Like | Cell differentiation | −2.01 | *** |
| ENSCARG00000013623 | *Sox7* | Transcription Factor Sox-7-Like | Cell differentiation | −0.62 | * |
| ENSCARG00000058624 | *Sox8* | Transcription Factor SOX-8-Like | Cell differentiation, sex differentiation | 0.91 | *** |
| ENSCARG00000041319 | *Tgf-βr2a* | Transforming Growth Factor Beta Receptor 2a | Cell growth and differentiation | −2.38 | *** |
| ENSCARG00000002050 | *Tgf-β3* | Transforming Growth Factor Beta Receptor Type 3-Like | Cell growth and differentiation | −0.52 | ** |
| ENSCARG00000020480 | *Tgf-β3* | Transforming Growth Factor Beta Receptor Type 3-Like | Cell growth and differentiation | 0.85 | ** |
| ENSCARG00000041319 | *Tgf-β1a* | Transforming Growth Factor Beta-1-Like | Cell growth and differentiation | −2.38 | *** |
| Continued | | | | | |

| Ensembl ID | Gene name | Gene description in Ensembl | Function | L2fc | padj |
|---|---|---|---|---|---|
| ENSCARG00000026896 | *Tgf-β5* | Transforming Growth Factor Beta-2-Like | Cell growth and differentiation | −0.94 | *** |
| ENSCARG00000035583 | *Tgf-βr2* | Transforming Growth Factor Beta receptor-2-Like | Cell growth and differentiation | 0.73 | * |
| ENSCARG00000023131 | *Thsd4* | Thrombospondin Type 1 Domain Containing 4 | TGF-β signalling | −2.07 | ** |
| ENSCARG00000008641 | *Thsd7* | Type 1 Domain Containing 7 | TGF-β signalling | −1.61 | *** |
| ENSCARG0000009933 | *Ugt8* | UDP-glucuronosyltransferase 8 | Steroid biosynthesis | −2.09 | *** |

**Table 5**. List of differentially expressed genes associated with signalling pathways and hormone biosynthesis between temperature-induced males and genotypic males. The gene function follows the biological databases Uniprot, KEGG, Zfin and GeneCards. Positive log2 fold change (l2fc) indicates transcripts that were more abundant in genotypic males. Negative log2 fold change indicates transcripts that were more abundant in temperature-induced triploid males. Asterisks indicate significant differences in gene expression level between genotypic and induced males: * for padj < 0.05, ** for padj < 0.01, *** for padj < 0.001.

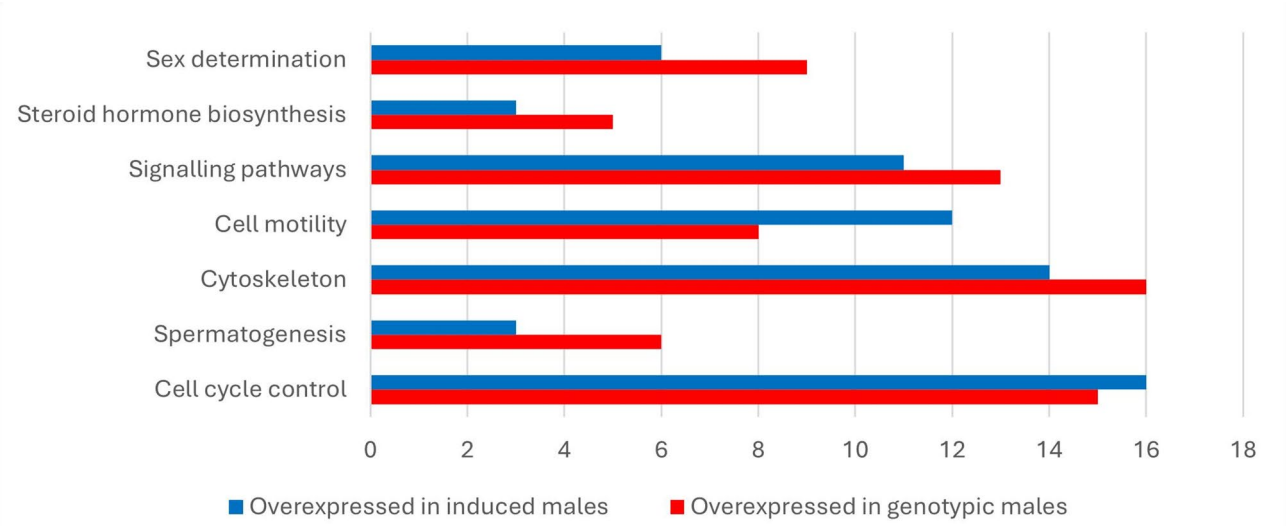


**Fig. 6**. Summary of reproduction-related differently expressed genes between genotypic and induced males of *C. gibelio*.

families dynein (*dync1i1*, *dnah5*, *dnai3*, *dnal1* and *dnal4a*), kinesin (*kif5ba*, *kif11*, *kif23* and *kif26aa*), and myosin (*myo3b*, *myo5aa* and *myo7ab*) (Supplementary Fig. 3).

## Signalling pathways

Several genes involved in signalling pathways related to cell differentiation and male determination were differentially expressed between genotypic and induced males (Table 5, Supplementary Fig. 4). Genes more highly expressed in induced males included members of the TGF-β superfamily, such as *tgf-β1*, one gene copy of *tgf-β3*, *tgf-β5*, the activin receptor family member *acvr2ba*, *thsd4* and *thsd7* (*thrombospondin domain containing proteins 4* and *7*), *bmp8* (*bone morphogenic protein 8*), *ltbp1* (*latent-transforming growth factor beta-binding protein 1*), the members of the follistatin family of BMP inhibitors *fstl1* and *fstl5*, and *smad4*. Conversely, transcripts of *smad3* and *smad7*; the TGF-β superfamily member *gsdf (gonadal soma derived factor)*, *bmp2*, *bmp5*, *bmp7*, *bmp10*, and *skilb* (ski-related novel protein N) were more highly expressed in genotypic males (Supplementary Fig. 4). Members of the Ras GTPase family showed contrasting patterns: *rasal1b* was more highly expressed in genotypic males, whereas *rasal3*, *rassf7b* and *hrasb* were more expressed in induced males.

## Hormone biosynthesis

Several genes involved in steroid hormone biosynthesis were differentially expressed between genotypic and induced males (Table 5, Supplementary Fig. 5). Genotypic males overexpressed several members of the cytochrome P450 superfamily, such as *cyp19a1a* (ovarian aromatase, estrogen synthetase), *cyp17a2* (steroid 17-alpha-monooxygenase, EC 1.14.1419) and *cyp7a1* (cholesterol-7-alpha-monooxygenase, EC 1.14.1423), as well as *srd5a2* (3-oxo-5-alpha-steroid 4-dehydrogenase 2, EC 1.3.1.22) and *comta* (catechol O-methyltransferase, EC 2.1.1.6) (Table 5). In contrast, induced males showed higher expression of *hsd17b2* (hydroxysteroid 17-β-dehydrogenase, EC 1.1.1.62), *ugt8* (UDP-glucuronosyltransferase 8, EC 2.4.1.17), and *chst6* (carbohydrate sulfotransferase 6, EC 2.8.2.2) (Table 5, Supplementary Fig. 5).

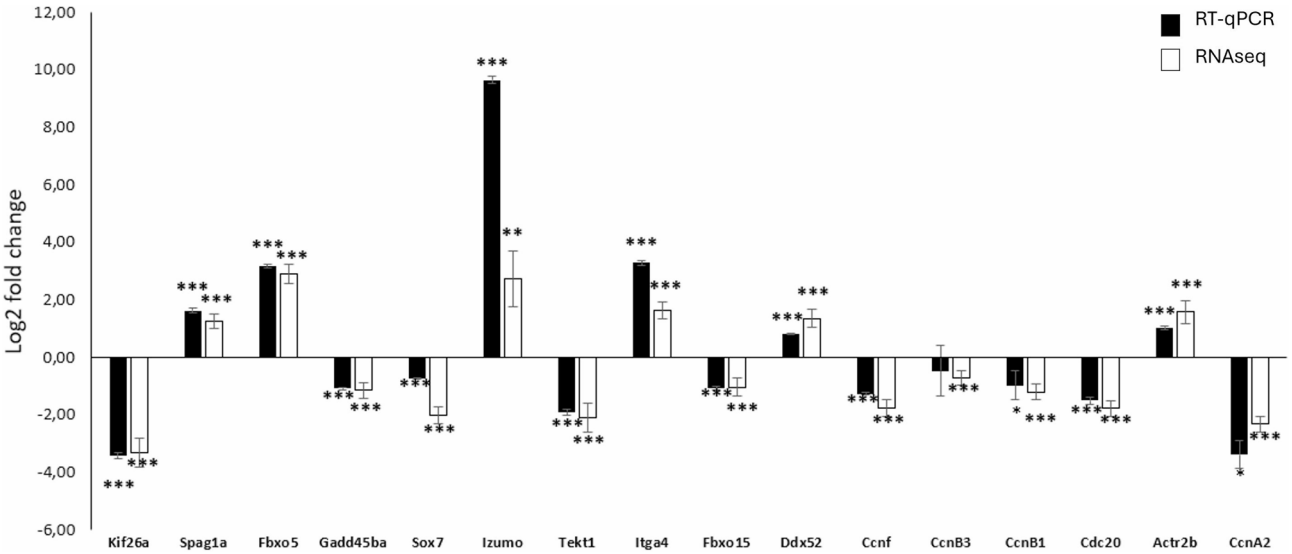


**Fig. 7**. Validation of gene expression resulting from RNA-seq by the RT-qPCR approach using 16 reproduction-associated genes. The x-axis displays the gene names. The y-axis displays the log2 fold change of the gene expression between genotypic males and temperature-induced males of *C. gibelio*. A positive log2 fold change in the gene expression indicates that the gene was upregulated in genotypic males compared to temperature-induced males. A negative log2 fold change indicates that the gene was downregulated in genotypic males compared to temperature-induced males. The data represents the means of five independent biological replicates, and bars represent standard deviation. Asterisks indicate statistically significant differences in the log2 fold change between the two male sex determination systems of *C. gibelio* based on Student's t-test: *$p < 0.05$, **$p < 0.01$, ***$p < 0.001$.

## Expression of sex determination genes between male groups

We compared transcriptional regulation of the set of sex-determination genes between genotypic diploid males and each group of temperature-induced males (Table 6): (1) male group 1 – triploid neomales resulting solely from full sex reversal at high temperature; (2) male group 2 – triploid males resulting from full sex reversal induced by high temperature, from a gynogenetic female whose offspring showed a high proportion of sex reversal at 22 °C and full sex reversal at 28–31 °C; (3) male group 3 – triploid males resulting from high proportional sex reversal induced by low temperature, from a gynogenetic female whose offspring showed a high proportion of sex reversal at 22 °C and full sex reversal at 28–31 °C.

When considering all induced male groups together, genotypic diploid males showed higher expression of *cyp19a1a* (cytochrome P450 aromatase), *sox8a* (SRY-box transcription factor 8), *gsdf* (gonadal soma-derived factor), and *lhx9* (LIM homeobox family 9) (Table 6). When expression patterns were analysed separately for each temperature-induced male group, consistent differences were observed for *cyp19a1a*, *gsdf*, *igf1*, *lhx9* and *sox8a*, which were more highly expressed in genotypic males compared to all three induced groups. However, *sox9b*, *amh*, *fshr* and *gata4* were significantly more expressed in genotypic males compared to induced males from groups 2 and 3 (involving both high- and low-temperature sex reversal) but not compared to males from group 1.

Additional differences were detected for eleven other genes. Among them, *dmrt2b*, *gdf6a*, *rspo1* (one paralogue), *sf1/nr5a1a* and *wt1a* were more highly expressed in induced males from group 1 compared to genotypic males, while four other genes showed differential expression only between genotypic males and males from group 3. *Dmrt2a* displayed an opposite pattern, being upregulated in males of group 1 and downregulated in males of group 3 relative to genotypic males.

## Validation of gene expression by RT-qPCR

To validate the differential expressions revealed by RNA-seq, we performed RT-qPCR on 16 selected differentially expressed genes involved in reproduction that were differently regulated between genotypic diploid males and temperature-induced triploid males of *C. gibelio* (Table 7). RT-qPCR analyses confirmed RNA-seq data on the downregulation of 10 reproduction-associated genes and upregulation of 6 reproduction-associated genes in genotypic males (Fig. 7).

## Discussion

Genotypic sex determination and, occasionally, temperature sex determination, exist in teleost fish, with various intermediate conditions. Both systems coexist in wild populations of the invasive cyprinid *C. gibelio*, although GSD is more frequent[31]. In this study, we compared the transcriptomes of testis tissues from gibel carp. We hypothesized that the expression of reproduction-related genes in males differs depending on genotypic and temperature-induced male sex determination. We analysed the differential expression of reproduction-related

| Gene name | Male group 1 | Male group 2 | Male group 3 |
|---|---|---|---|
| *Amh* | 0.61 | 1.03* | 1.40* |
| *Cirbpa* | −0.51 | −0.47 | −0.75* |
| ***Cyp19a1a*** | **2.55*** | **2.27*** | **2.69*** |
| *Dmrt1* | 0.22 | 0.14 | 0.12 |
| *Dmrt1* | −0.19 | −0.07 | 0.02 |
| *Dmrt2a* | −0.75* | 1.20 | 1.55* |
| *Dmrt2a* | 0.00 | 0.52 | 0.49 |
| *Dmrt2b* | −0.60 | 0.98 | 1.26* |
| *Dmrt2b* | −1.21* | −0.32 | −0.17 |
| *Dmrta2* | 0.21 | 0.31 | 0.42 |
| *Foxl2b* | −0.47 | 0.13 | −0.25 |
| *Foxl2b* | −0.47 | 0.13 | −0.25 |
| *Fshr* | −0.23 | 0.69* | 0.90* |
| *Gata4* | 0.61 | 1.43* | 1.22* |
| *Gdf6a* | −1.36* | −0.37 | −0.71 |
| ***Gsdf*** | **0.92*** | **1.52*** | **1.49*** |
| ***Igf1*** | **−1.67*** | **−1.12*** | **−1.68*** |
| ***Lhx9*** | **1.88*** | **2.48*** | **2.77*** |
| *Nr0b1(Dax1)* | −0.11 | 0.85 | 0.84* |
| *Rspo1* | −1.16* | −0.27 | −0.07 |
| *Rspo1* | −0.43 | 1.28 | 1.48* |
| *Sf1 (Nr5a1a)* | −0.65* | −0.30 | −0.43 |
| ***Sox8a*** | **0.88*** | **1.52*** | **1.56*** |
| *Sox9b* | 0.61 | 1.09* | 0.97* |
| *Star* | 1.13* | 1.02 | 1.15* |
| *Wt1a* | −0.88* | −0.54 | −0.09 |

**Table 6**. List of male determination genes with their differential expression levels between genotypic and induced males. Three different groups of temperature-induced males are considered (group 1: full sex reversal at 28–31 °C, group 2: sampled at 28–31 °C from the offspring of a female with high sex reversal proportion at 22 °C and full sex reversal at 28–31 °C, group 3: sampled at 22 °C from the offspring of a female with high sex reversal proportion at 22 °C and full reversal at 28–31 °C). Differences in expression are indicated by the log2fold change. Positive log2 fold change (l2fc) indicates transcripts that were more abundant in genotypic males. Negative log2 fold change indicates transcripts that were more abundant in temperature-induced males. Bold indicates the genes with significant differences in gene expression level between genotypic males and each group of induced males (padj < 0.05). Asterisks indicate significant differences in gene expression level between genotypic and induced males of a given group (padj < 0.05).

genes in genotypic diploid males and temperature-induced triploid males. The transcriptome profiles of testes based on normalized RNA-seq read counts differed between the two male categories, with little to no difference between the three groups of temperature-induced males. GO and KEGG analyses highlighted pathways related to meiosis (DNA recombination, regulation of meiotic cell cycle) and spermatogenesis (microtubule binding and movement, motile cilium) as enriched in genotypic males. Furthermore, we identified more than 150 genes related to meiosis, spermatogenesis, sex differentiation, hormone signalling, and fertilization that were differentially expressed between TSD and GSD males. Altogether, our results suggest that sex differentiation processes differ between temperature-induced males and genotypic males, and that genotypic males maintain a more efficient regulation of meiotic progression and spermatogenesis.

We compared gene expression levels for an exhaustive set of 40 meiosis-specific genes inferred from previous studies[52–56]. Most of them showed similar expressions across groups, but genotypic males slightly upregulated *mlh1*, involved in recombination and crossover, suggesting more efficient homologous recombination in genotypic males, although temperature-induced males upregulated *smc4*, the recombinases *rad51c*, *rad51b* and *rad52*, and *mitotic arrest deficient 2 like 2 (mad2l2)*. Ras GTPase family genes, such as *rasal1b* and *rasal3*, involved in cell division control, growth and differentiation[57–61], and meiosis regulation[62], were also differentially expressed, as well as FGF (fibroblast growth factor) family genes, and related proteins (fibroblast receptor, fibroblast binding proteins), sperm maturation regulators especially expressed in male gonads[63] and involved in male differentiation in platyfish[64]. Taken together, these results suggest differences in cell cycle control and meiosis between genotype-determined diploid and temperature-determined triploid males of *C. gibelio*. However, ploidy changes often affect meiosis, including double-strand break repair and synaptonemal complex formation[65,66].

Our study suggests differences in sex differentiation processes between TSD and GSD. Genes of the SRY-box (*sox*) transcription factor family, major actors in gonadal development[67], were differentially expressed

| Gene name | Full name | Gene ID | forward/reverse primers (5'->3') | Amplicon size |
|---|---|---|---|---|
| *Ccna2* | Cyclin A2 | ENSCARG00000044731 | AATACAAGGGCTCAAAGTACCA | 197 |
| | | | AAGATCTCACCATTTCCCCAAA | |
| *Fbxo5* (*emi1*) | F-box Protein 5 | ENSCARG00000056526 | GGAGATTGTGACTTAGTGAGCTGT | 138 |
| | | | TAATGAGCCCATGAGGCGAC | |
| *Actr2b* | Activin receptor type-2B | ENSCARG00000061469 | CGTCAAGAAGGGATGCTGGT | 166 |
| | | | AGGAGACTCCAGCACTGGTC | |
| *Cdc20* | Cell division cycle protein 20 homolog | ENSCARG00000027165 | CCCAGCAAAACACCAGGAAAG | 164 |
| | | | GGTGCTGTAGTGGATGCGA | |
| *Ccnb1* | Cyclin B1 | ENSCARG00000028136 | AACCTCAGCGCACAATCAGT | 129 |
| | | | CAGGCGAGTGTTCCTTGAGA | |
| *Ccnb3* | Cyclin B3 | ENSCARG00000062532 | GGACTGGAGAACCAGGATGG | 109 |
| | | | CAATCTTGTGTGCATTTGTGATGT | |
| *Ccnf* | Cyclin F | ENSCARG00000060407 | TCACTGTGAAGCATTATTGTTGAA | 75 |
| | | | ACAGTGGAGCACGCCC | |
| *Spag1a* | Sperm associated antigen 1a | ENSCARG00000007149 | CACACAAAGGCTTGAAGGACTAT | 171 |
| | | | TTCATCCTTTATTGCCTAGATGTCA | |
| *Ddx52* | Dexd-Box Helicase 52 | ENSCARG00000010183 | GATTCATGCGGATCGCACAC | 194 |
| | | | CTCTTCCAGTTCGCCCGAT | |
| *Gadd45ba* | Growth arrest and DNA-damage-inducible, Beta a | ENSCARG00000056928 | ACTGCATCATAGTCACTAACCCT | 159 |
| | | | TCATTGCATCAAAAGCATAGCAGT | |
| *Fbxo15* | F-box protein 15 | ENSCARG00000037330 | GTGCCACTCAATTGTCCTGC | 167 |
| | | | ATTCCCCACTGGTCCTTCCA | |
| *Tekt1* | Tektin 1 | ENSCARG00000062861 | GATTGGCAGCAGTTGACAGAAAAA | 105 |
| | | | CGAGCTCCTGAAATGCACCT | |
| *Kif26a* | Kinesin family member 26a | ENSCARG00000043633 | CTGTGCACGCTCCACCTCTT | 184 |
| | | | GGTGTAGCTTTTGCCGAGGT | |
| *Itga4* | Integrin subunit alpha 4 | ENSCARG00000023759 | TGATTTCATCACTACCCTCTAGACA | 197 |
| | | | TCCAACCATCAGCCATGTGT | |
| *Sox7* | Sry-box transcription factor 7 | ENSCARG00000050582 | CTGAGCAAGATGCTGGGAAAG | 138 |
| | | | CTTCTTCCTACGAGGACGGT | |
| *Izumo* | Izumo sperm-egg fusion protein 1 | ENSCARG00000049815 | GGAGAGCATCATCTCGAGGC | 140 |
| | | | TCCCCGTCTTGTGACAGATTC | |

**Table 7**. List of the target genes selected from RNA-seq analysed using RT-qPCR. Their respective primer sequences and amplicon size are indicated.

in genotypic males and temperature-induced males. *Sox9b* is involved in sex reversal and was reported to be downregulated in temperature-induced masculinized zebrafish[68]. *Sox9* was more expressed in genotypic males than in males resulting from sex reversal at both high and low temperatures (male groups 2 and 3) but not compared to males that were induced only at high temperature. Most importantly, genotypic males overexpressed *sox8*, involved in testes differentiation in teleost fish[67,69–71] and other animals[72]. *Sox8*, expressed in Sertoli cells[73], participates in testis differentiation by activating 3b-hydroxysteroid dehydrogenase, *cyp19a1a*, *amh* and *dmrt1*, and by repressing female pathway genes[70,72,74], with functions partly overlapping *sox9* which it may substitute[69]. Conversely, temperature-induced triploid males upregulated the ovarian development regulator *sox7*, involved in female differentiation in fish[67,73]. However, temperature-induced males did not upregulate the ovarian development regulator *foxl2b*, contrary to groupers (*Epinephelus coioides*♀ × *E. lanceolatus*♂)[75]. These differences might be due to temperature-induced males of gibel carp being obtained from gynogenetic females.

*Dmrt1*, a homologue of the Y-specific male-determining gene *dmy* of *D. rerio*[17] that plays a key role in temperature-induced gonad differentiation in a way similar to the SRY factor of mammals[76–78], was not differentially expressed between male groups, contrary to what was reported in Nile tilapia[79]. The differential expression of this gene could be more pronounced in earlier stages of embryonic development, as previously reported[50,80]. However, genotypic males overexpressed other *dmrt* family members, such as the male-specific *dmrta2*, that regulates spermatogenesis and sex determination[81,82] and neurogenesis in fish[83,84]. Furthermore, on a set of 26 genes, 15 showed transcriptional differences among induced male groups, including the major sex-determining genes *gsdf*, *rspo1*, *fshr*, *wt1* and *cirbpa*. This suggests complex molecular mechanisms of TSD in gibel carp, and varying sex reversal potential at a given temperature between offspring of gynogenetic females.

The Sox9-Amh-Cyp19a1 regulatory cascade is crucial to male differentiation[85]. Genotypic males strongly overexpressed the gonad-specific *cyp19a1a* compared to all three temperature-induced male groups. This gene encodes the oestrogen synthetase, involved in steroidogenesis[86] and gonadal differentiation, whose activity inhibition induces female-to-male sex reversal[87]. This result contrasts with what was reported in Nile

tilapia[88,89], Atlantic halibut (*Hippoglossus hippoglossus*)[90] and Japanese flounder (*Paralichthys olivaceus*)[87], where temperature-induced males upregulated *cyp19a1a*, as well as triploid serranid hybrids (*Epinephelus coioides*♀ × *E. lanceolatus*♂) in comparison to diploid hybrids[75]. Genotypic males upregulated *amh*, encoding the anti-Müllerian hormone, which is activated by *sox9* in the Sertoli cells and plays a major role in testis differentiation and spermatogenesis in fish[91]. Its transcription level depends on 17β-estradiol and *cyp19a1*[92–94]. In fish with pronounced temperature-dependent sex determination, *amh* expression was reported to be higher at masculinizing than at feminizing temperatures during the gonadal differentiation period[80], but an increase in *amh* expression could be a consequence of sex differentiation rather than its cause[95]. Our data support the proposed functions of *sox8* and *amh* in TSD-induced masculinization in fish[75], but contrast with the reported downregulation of these genes in the gonads of temperature-induced males of *Tilapia* compared to the genotypic males[79].

Androgens and oestrogens are central for sex differentiation and gonad development. In our study, genotypic males of gibel carp upregulated *star*, encoding the steroidogenic acute regulatory protein, involved in cholesterol intracellular transport for steroid biosynthesis[96]. They also slightly upregulated the germ cell maintenance gene *piwil2*, an Argonaute family member involved in male fertility and spermatogenesis. The markers related to this gene were suggested for useful sex identification in gonochoristic fish species with no sexual dimorphism[97].

In contrast, genotypic males slightly downregulated the Sertoli and Leydig cells specific gene *sf1* (steroidogenic factor 1)[98], linked to male gonad differentiation, only compared to temperature-induced males with only full sex reversal at 28–31 °C. This gene regulates sex determination genes such as *amh*[47] and androgen receptors[99], and was also reported to be expressed in turtles with TSD[100]. In our study, steroid hormone synthesis genes and pathways were also differentially regulated, such as *hsd17b2*, which was strongly upregulated in temperature-induced males. This gene encodes hydroxysteroid 17-β-dehydrogenase, a key regulator of sexual differentiation and sex reversal in fish[101,102], which oxidizes estradiol and testosterone to mitigate their action.

Components of the TGF-β pathway, a major signalling pathway that controls many physiological processes in animals[103,104], including sexual differentiation in fish[105–107], were found to be differentially expressed between genotypic and temperature-induced males. Specifically, several members of the TGF-β family (*tgf-β1*, *3*, *5*) and latent TGF-β (*ltbp1*), as well as *smad4*, that acts downstream of the TGF-β signalling pathway[108], were downregulated in genotypic males. The female-specific oocyte differentiation regulator *rbpms2b*[109,110] was more expressed in temperature-induced males. In contrast, genotypic males upregulated the negative TGF-β signalling controller *skilb*[111], the gene encoding the activin receptor *actr3b*, as well as the male-differentiation gene *gsdf* (*gonadal soma-derived factor*), involved in testes differentiation and androgen-induced sex reversal cascade in fish[112–114]. Altogether, these results suggest that steroid signalling and regulation differ between genotypic and temperature-induced males.

Temperature-induced males overexpressed several myosin-encoding genes, members of the actin-related protein 2/3 complex (*arpc1b*), the diaphanous-related formin 3 (*diaph3*, involved in cytokinesis at high temperatures[115], and gelsolin (*gsn*). In addition, members of the tektin family, such as *tekt1* and *tekt4*, expressed in testes and involved in the formation of flagellar microtubules of the sperm cells[116,117], were more expressed in temperature-induced males. Inversely, *spag1a* and *sperm flagellar 2* (*spef2*), involved in axoneme assembly and structural integrity[118], were more expressed in genotypic males. The downregulation of these genes in temperature-induced males suggests reduced fertility compared to genotypic males, likely due to lower sperm motility, and supports previous reports of impaired fertilization ability in sperm from TSD gibel carp males[33].

Several major actors in egg fertilization were differentially expressed between genotypic diploid and temperature-induced triploid males of gibel carp. Our results highlight the role of *izumo* in genotypic gibel carp males; this gene, encoding the sperm-specific protein Izumo of the acrosome, is important in sperm-egg fusion due to its conjugation with the egg-specific Juno[119]. Other cell adhesion-encoding genes, such as *cd9a* and *b*, were also differently regulated between genotypic and induced males of gibel carp. CD9 proteins, present on the sperm surface, participate in sperm binding to the zona pellucida of the egg[120,121]. It is noteworthy that paralogues (genes belonging to the same family, resulting from gene or genome duplication[122]) could be differently regulated between gynogenetic and temperature-induced males. For instance, *cd9a* was downregulated in genotypic males while *cd9b* was upregulated, as well as calmodulin kinases and members of the TGF-β pathway. This suggests subfunctionalization following gene duplication, in accordance with previous studies on this gene[123]. GO terms and KEGG pathways related to cell-cell adhesion were also overrepresented in genotypic males, such as integrin complex and cell adhesion. Several members of the integrin family, conserved transmembrane glycoproteins involved in cell-cell and cell-extracellular matrix as well as signal transduction[104,124], such as *itga2*, *4*, *6* and *8*, were upregulated in genotypic males. They play important roles in sperm maturation and migration processes, sperm-egg adhesion and acrosome reaction during fertilization in vertebrates[125]. All these results suggest differences in spermatogenesis regulation, sperm motility and fertilization processes between males of gibel carp resulting from GSD and TSD. Consistently with our results, genes associated with sperm flagellum assembly and motility, including members of the dynein family (*dnad*, *dnai* and *dnald*), genes encoding tektins, *spag*, and *spef2* were previously reported to be differentially expressed in the testes of diploid and sterile triploid males of *C. auratus*[116]. Our results suggest differences between genotypic and temperature-induced males concerning spermatogenesis and sperm-egg binding. The downregulation of spermatogenesis genes *spag1a* and *spef2* and the fertilization gene *izumo* highlights the reported impaired reproductive abilities of temperature-induced males of gibel carp, which was originally proposed on the basis of the different sperm nucleus behaviours of genotypic and temperature-determined males[33].

In our study, we investigated the temperature-induced sex reversal from females to males in the offspring of gynogenetic females resulting from asexual reproduction. Following egg activation of gynogenetic females by heterologous or homologous sperm, the males were reared until the adult stage and two scenarios were observed: (1) all females offspring at 22 °C, partial sex reversal (low proportion of males) at 25 °C, and full

reversal to males from 28 °C (male group 1), or (2) partial sex reversal (high proportion of males) at 22 °C (male group 3), a high proportion of males or full reversal at 25 °C, and full reversal to males at 28–31 °C (male group 2). Our results are in accordance with previous studies suggesting that temperature modulates gonad differentiation and causes sex reversal in gynogenetic *C. gibelio*, and may influence the sex ratio in gibel carp populations under varying water temperatures[31]. Specifically, Li et al.[31] showed that male incidence in laboratory gynogenetic *C. gibelio* progenies increased with increasing larval rearing temperature. However, the presence of induced males even at low temperature suggests that other environmental factors could trigger female-to-male sex reversal, the pattern previously suggested for *Carassius auratus*[126]. Histological analysis of laboratory-reared and wild specimens revealed similar testis morphology in genotypic and temperature-induced males of gibel carp, regardless of ploidy. In *C. gibelio*, males resulting from GSD and TSD do not display the same reproductive abilities, and only genotypic males produce sperm cells that are able to fuse with the female pronucleus[33]. For this reason, we compared the expression regulation of genes involved in spermatogenesis and fertilization between genotypic males and temperature-induced males. Spermatogenesis includes three distinct steps: mitosis, meiosis and spermiogenesis, an important specialization of sperm cells, that develop specific organelles: the acrosome and the flagellum, requiring important cytoskeleton reorganization[127] to form an axoneme of microtubule, associated with molecular motors of the dynein family. Other molecular motor and components of the cytoskeleton, such as kinesins[128], actin and myosin, are critical for sperm cell differentiation, including acrosome biogenesis and vesicle transport[129].

*Carassius gibelio* likely originated from a triploidization event in *C. auratus*[25,26,130], with a potential genetic contribution of *C. carpio*[46,131]. Following initial invasion, *C. gibelio* populations were composed of triploid females only, reproducing asexually by gynogenesis[21]. The later re-acquisition of sexual reproduction and the appearance of males, a unique case in asexual species, led to the coexistence of sexual and gynogenetic individuals in the same populations of *C. gibelio* in Asia and Europe[41,132]. The former explanation of the minor presence of males in the populations of all gynogenetic female populations was based on the assumption that gynogenetic triploid females exhibit two kinds of reproduction – asexual, when using heterologous sperm for the activation of eggs and embryo development, or sexual, when using homologous sperm[132]. In fact, many sexual reproduction-related genes are maintained and expressed in gynogenetic females of gibel carp, suggesting that these females retain the genetic toolkit for meiosis and sexual reproduction[46]. However, our experimental breeding showed that some gynogenetic females produced solely triploid female offspring, and that the appearance of triploid males was only induced by high temperature, whilst other gynogenetic females may produce males already at a lower temperature. This suggests that supplementary environmental or genetic components may also be involved in sex determination of male offspring of gynogenetic females. However, several field studies in European waters have documented triploid-diploid populations of gibel carp with about 37–60% females, reproducing mostly by gynogenesis, and 40–63% of diploids with the same female: male ratio. Triploid males have rarely been reported in nature[133,134], in support of the hypothesis that temperature-induction of triploid males currently plays a greater role in the appearance of triploid males than the sexual reproduction of gynogenetic females.

The results of the present study shed new light on the evolution of the asexual and sexual complex of gibel carp. These findings suggest that using both gynogenetic and sexual reproduction allows gibel carp, a very successful invasive species across European countries, to combine the advantages of gynogenetic reproduction, which affords especially fast population growth[135], with the advantages of sexual reproduction, which provides higher resistance to parasites, higher aerobic performance, and better immunity compared to gynogenetic females[136]. The extreme plasticity of gibel carp, combining gynogenesis and sexual reproduction, as well as the possibility of temperature-induced sex reversal, highlights its unique evolutionary trajectory and likely explains the high ecological tolerance and invasiveness of this species in European aquatic ecosystems.

## Conclusion and perspectives

Our transcriptomic comparisons suggest significant differences between genotypic and temperature-induced male differentiation in *C. gibelio*. Induced males show underrepresentation and lower expression of meiotic regulators and genes controlling cell cycle checkpoints and homologous recombination, which may impair the accuracy of meiosis and provide a mechanistic explanation for their lower reproductive abilities. Genotypic male differentiation is associated with several major sex determination genes, including *sox8*, *gsdf*, and *lhx9*, as well as hormone synthesis genes such as *amh* and *cyp19a1a*. Temperature-induced masculinization is associated with transcriptional activation of *hsd17b2*, involved in steroid biosynthesis, and the meiotic gene *mnd1*. Our results also confirm the central role of *cyp19a1* in sex determination and suggest that this gene plays a major role over a wider range of temperature-induced female-male sex reversal in *C. gibelio*. The downregulation of critical genes involved in cytoskeletal assembly and flagellum function, and sperm-egg interaction, highlights the impaired spermatogenesis, reduced functional sperm motility and fertilization abilities of temperature-induced males. At the hormonal level, the lower expression of genes involved in male differentiation, *sox8*, *amh* and *cyp19a1a*, in temperature-induced males, suggests differing male sex-differentiation pathways between GSD and TSD. Our findings contribute to the understanding of the molecular mechanisms responsible for the coexistence of sexual and asexual forms of gibel carp populations. Future integrative research combining transcriptome profiling with functional assays, such as sperm motility tests, fertilization success, hormone quantification, and histological analyses of spermiogenesis, could link differential expression of meiosis and spermatogenesis genes with reproductive capacity, to provide deeper insight into the evolution of sex and males within all-female asexual species.

## Materials and methods

Specimens of *C. gibelio* were generated from the artificial breeding of fish that were sampled in the Dyje River (Czech Republic) and genotyped according to published studies[133,134,137]. Ploidy was determined using a Partec CCA-I flow cytometer (Partec GmbH)[136] using diploid *C. auratus* as standard. *Carassius gibelio* specimens collected from the wild and used for artificial breeding were separated according to sex into two well-aerated tanks and stimulated for ovulation/spermiation by carp pituitary. Oocytes of ovulating females and sperm were sampled according to Gela et al.[138]. We performed the sexual crossing (diploid females and diploid males) and the induced gynogenesis (using sperm of diploid male *C. gibelio*, *C. carpio* or *A. brama* for induction of gynogenesis). Following published studies[31], the embryos were incubated at 22 °C during the periods of embryogenesis and larval hatching, and then the larvae were reared in aquaria with oxygenated water at a temperature of 22 (± 0.5) °C. For temperature influence on male determination, we randomly selected 400 larvae derived from the eggs of the each gynogenetic female, then larvae from the same gynogenetic female until first feeding were divided into groups and the rearing temperature was gradually changed from 22 (± 0.5) °C to 25 (± 0.5), 28 (± 0.5), and 31 (± 0.5) ℃, respectively. The larvae were reared in aquaria with oxygenated water for 35 days, then the temperature gradually decreased to 22 °C. The larvae were fed with live artemia, subsequently frozen adult artemia and commercial dry pellet. Fish offspring were reared in aquarium conditions until two years of age (i.e., sexual maturity) before their gonadal tissues were collected. Fish sex was determined visually for offspring of each female corresponding the different temperature treatments (i.e., sex was determined for 100 offspring at 22 °C, 100 offspring at 25 °C, 100 offspring at 28 °C, and 100 offspring at 31 °C of each female) based on the presence of ovaries or testes.

Gonadal histology was performed on subsets of genotypic males and temperature-induced males from the experimental breeding, as well as on sexual diploid males and rare triploid males collected from the wild. Paraffin histology techniques applied in the study followed the standard procedure described in Bancroft's Theory and Practice of Histological Techniques[139]. Two types of fixatives (Davidson's fluid according to the original recipe and its modified version[94] specifically for male gonads) were used; 3–4 µm thick sections were stained with hematoxylin and eosin. On the basis of light microscopy, male gonads were assigned into reproductive classes defined from the literature[45].

First, analyses focused on reproduction-associated genes and meiosis-associated genes in genotypic diploid males (resulting from artificial sexual reproduction) and temperature-induced males were performed (see below). Next, analyses focused on sex-determination genes were performed. We selected the groups of temperature-induced males based on the pattern observed for sex reversal in the offspring of gynogenetic females. For the gynogenetic females we observed either (1) no sex reversal at 22 °C, weak sex reversal at 25 °C and full sex reversal at 28 °C and 31 °C, or (2) moderate to high sex reversal at 22 °C, high sex reversal at 25 °C and full sex reversal at 28 and 31 °C. As the objective of this part of the study was to compare the DEGs linked to male sex determination between genotypic and temperature-induced males, we selected the male offspring corresponding to (1) full sex reversal at 28 °C and 31 °C only (termed as male group 1), (2) high sex reversal at 22 °C (termed as male group 3) and (3) full sex reversal at 28 °C and 31 °C (termed as male group 2) for the offspring of the same gynogenetic females in which a high sex reversal of offspring was recorded already at 22 °C. Then, we compared the genotypic diploid males and each of these three temperature-induced male groups.

Fish were euthanized by physical stunning through a blow to the skull with a blunt wooden instrument immediately followed by exsanguination. Gonadal tissues were submerged in Ambion RNAlater stabilization solution (Thermo Fisher Scientific, Waltham, MA, USA) and stored at −80 °C until the isolation of total RNA. Prior to sampling, the ploidy of each *C. gibelio* specimen was checked using the same methodology as described above.

### RNA extraction and library preparation

Testes RNA was isolated with the PureLink® RNA Mini Kit (Ambion) combined with Trizol reagent (Thermo Fisher Scientific, Waltham, MA, USA), including PureLink DNase treatment, following Jacques et al.[46]. RNA concentration was measured with a QubitTM 4 fluorometer (Invitrogen by Thermo Fisher Scientific, Waltham, MA, USA) and Qubit RNA HS Assay Kit (Thermo Fisher Scientific, Waltham, MA, USA). RNA quality was assessed with the RNA 6000 Nano Kit and 2100 Bioanalyser (Agilent Technologies, Santa Clara, CA, USA). RNA integrity (RIN) was subsequently measured in an external genomic facility using a Fragment Analyzer and RNA Kit 15 nt (Agilent Technologies). RNA enrichment and full-length RNA-seq libraries were prepared using the NEBNext Poly(A) mRNA Magnetic Isolation Module (New England Biolabs) and NEBNext Ultra II Directional RNA Library Prep Kit (New England Biolabs) with xGen™ CS adapters (IDT) containing UMIs, respectively. The sequencing was performed on a NovaSeq 6000 (Illumina) in paired end 150 bp mode.

### NGS data analyses

The quality of raw fastq reads was analysed using FastQC[140] and BioBloomTools v.2.3.4 following Jacques et al.[46]. The clipping of Illumina adapters and the quality trimming of raw fastq reads were realized with Cutadapt v.4.3 (-quality-base = 33 -q 0,20 -m 35 -M 250), and the mapping of trimmed RNA-seq reads was performed using *Carassius auratus* (ASM336829v1) as reference genome, using STAR v.2.7.3a[141] with default parameters except --outFilterMismatchNoverLmax 0.4 and --twopassMode Basic. Uniquely- and multi-mapped reads number and percentage, rRNA contamination, mapped regions, read coverage distribution, strand specificity and gene biotypes control were processed using RSeQC v.4.0.0[142], Picard toolkit v.2.25.6[143], and Qualimap v.2.2.2[144]. MultiQC v.1.10.1[145] was used for statistics.

### Differential expression analysis and pathway enrichment analysis

The bioinformatic processing of raw sequencing data was performed following Jacques et al.[46], using uniquely mapped read counted by featureCount from Subread package v.2.0[146] for differential gene expression calculation, the Bioconductor package DESeq2 v.1.34.0[147] for analysis with the formula: design = ~ condition, including the principal component analyses (PCA). IDEP 2.0[148] was used to generate the heatmap. Gene Ontology (GO) terms and KEGG pathways[149–152] enrichment were performed with David[153], using genes with baseMean > 10 as background and the criteria from Jacques et al.[46]. Significantly differentially expressed genes (DEGs) between testes of genotypic and temperature-induced males were selected based on the following criteria: baseMean > 10 and padj < 0.05. The molecular databases Uniprot[154], KEGG[150–152], Zfin[155] and GeneCards[156] were used to determine gene function, and KEGG was used to analyse the function of genes in specific biological pathways.

### Gene selection and real-time quantitative PCR

Twenty reproduction-associated genes were selected from RNA-seq data based on GO and KEGG terms and published studies[54–56,157] and were used for validation by RT-qPCR analysis. Two reference genes, A-tubulin (*A-tub*) and B-actin (*B-act*), were tested for their stability using qPCR on 12 samples representing the biological replicates for each group (genotypic males and temperature-induced males), following the conditions described below, and the ΔCq method. The two reference genes were considered stable based on standard deviation of ΔCq < 0.5 (0.204) and used for expression data normalization in our data set. Amplification specificity was assessed using classical PCR. Amplification efficiency (E = 90–110%) and regression coefficient ($R^2$> 0.98) were considered acceptable. The PCR was run under the following conditions: an initial denaturation at 95 °C for 10 min, followed by 40 cycles of 95 °C for 15 s and a gene-specific annealing temperature (AT, 54–57 °C) for 30 s, followed by 45 s at 72 °C. A melting curve analysis was performed to verify the PCR specificity (95 °C for 15 s, gene-specific AT for 1 min, and gene-specific AT to 95 °C gradually increasing by 0.5 °C per 5 s). The successful RT-qPCR was performed for 16 biologically relevant genes based on protocols published by Jacques et al.[46], and using the Reference Gene Selection Tool from Bio-Rad CFX Maestro software (Bio-Rad)[158]. As PCR amplified unspecific products for the other four reproduction-associated genes selected from RNA-seq, they were not included in qPCR. Primers were designed to cover exon-exon junctions, with the primer designing tool Primer Blast[159]. The selection of genes and their primer sequences are summarized in Table 7. The reverse transcription was performed using High-Capacity RNA-to-cDNA Kit (Applied Biosystems by Thermo Fisher Scientific). Classical PCR and RT-qPCR were performed following the protocols and conditions published by Jacques et al.[46]. Real-time qPCR was realized with LightCycler 480 II Real-Time PCR System (Roche Diagnostics) and LightCycler 480 SYBR Green I Master chemistry (Roche), using *A-tub* and *B-act* as housekeeping genes. RT-qPCR outputs were analysed using the ΔΔCq method[160] and genotypic diploid males as control group.

## Data availability

The data used in this study have been deposited in NCBI´s Gene Expression Omnibus and are accessible through the GEO Series accession number GSE285878 (https://www.ncbi.nlm.nih.gov/geo/query/acc.cgi? acc=GSE285878).

Received: 29 July 2025; Accepted: 3 November 2025
Published online: 25 November 2025

## References

1. Graves, J. A. M. Weird animal genomes and the evolution of vertebrate sex and sex chromosomes. *Annu. Rev. Genet.* **42**, 565–586 (2008).
2. Bachtrog, D. et al. Sex determination: why so many ways of doing it? *PLoS Biol.* **12**, e1001899 (2014).
3. Brown, E. E., Baumann, H. & Conover, D. O. Temperature and photoperiod effects on sex determination in a fish. *J. Exp. Mar. Biol. Ecol.* **461**, 39–43 (2014).
4. Warner, R. R., Fitch, D. L. & Standish, J. D. Social control of sex change in the shelf limpet, *Crepidula norrisiarum*: size-specific responses to local group composition. *J. Exp. Mar. Biol. Ecol.* **204**, 155–167 (1996).
5. Casas, L. et al. Sex change in clownfish: molecular insights from transcriptome analysis. *Sci. Rep.* **6**, 35461 (2016).
6. Shang, E. H. H., Yu, R. M. K. & Wu, R. S. S. Hypoxia affects sex differentiation and development, leading to a male-dominated population in zebrafish (*Danio rerio*). *Environ. Sci. Technol.* **40**, 3118–3122 (2006).
7. Baroiller, J. F., D'Cotta, H. & Saillant, E. Environmental effects on fish sex determination and differentiation. *Sex. Dev.* **3**, 118–135 (2009).
8. Robertson, C. E., Wright, P. A., Köblitz, L. & Bernier, N. J. Hypoxia-inducible factor-1 mediates adaptive developmental plasticity of hypoxia tolerance in zebrafish, *Danio rerio*. *Proc. R. Soc. B Biol. Sci.* **281**, 20140637 (2014).
9. Ospina-Álvarez, N. & Piferrer, F. Temperature-dependent sex determination in fish revisited: prevalence, a single sex ratio response pattern, and possible effects of climate change. *PLoS One.* **3**, e2837 (2008).
10. Conover, D. O., Van Voorhees, D. A. & Ehtisham, A. Sex ratio selection and the evolution of environmental sex determination in laboratory populations in *Menidia menidia*. *Evolution* **46**, 1722–1730 (1992).
11. Holleley, C. E. et al. Sex reversal triggers the rapid transition from genetic to temperature-dependent sex. *Nature* **523**, 79–82 (2015).
12. Devlin, R. H. & Nagahama, Y. Sex determination and sex differentiation in fish: an overview of genetic, physiological, and environmental influences. *Aquaculture* **208**, 191–364 (2002).
13. Wilson, C. A. et al. Wild sex in zebrafish: loss of the natural sex determinant in domesticated strains. *Genetics* **198**, 1291–1308 (2014).
14. Sarre, S. D., Georges, A. & Quinn, A. The ends of a continuum: genetic and temperature-dependent sex determination in reptiles. *BioEssays* **26**, 639–645 (2004).
15. Waters, P. D., Wallis, M. C. & Graves, J. A. M. Mammalian sex - origin and evolution of the Y chromosome and SRY. *Semin Cell. Dev. Biol.* **18**, 389–400 (2007).
16. Schroeder, A. L., Metzger, K. J., Miller, A. & Rhen, T. A novel candidate gene for temperature-dependent sex determination in the common snapping turtle. *Genetics* **203**, 557–571 (2016).

17. Matsuda, M. et al. *DMY* is a Y-specific DM-domain gene required for male development in the medaka fish. *Nature* **417**, 559–563 (2002).
18. Li, M. et al. A tandem duplicate of Anti-Müllerian hormone with a missense SNP on the Y chromosome is essential for male sex determination in Nile tilapia, *Oreochromis niloticus*. *PLoS Genet.* **11**, e1005678 (2015).
19. Chen, S. et al. Whole-genome sequence of a flatfish provides insights into ZW sex chromosome evolution and adaptation to a benthic lifestyle. *Nat. Genet.* **46**, 253–260 (2014).
20. Halačka, K., Lusková, V. & Lusk, S. *Carassius* '*gibelio*' in fish communities of the Czech Republic. *Ecohydrol. Hydrobiol.* **3**, 133–138 (2003).
21. Lusková, V., Lusk, S., Halačka, K. & Vetešník, L. *Carassius auratus gibelio* - the most successful invasive fish in waters of the Czech Republic. *Russ. J. Biol. Invasions.* **1**, 176–180 (2010).
22. Perdikaris, C. et al. *Carassius gibelio* in Greece: the dominant naturalised invader of freshwaters. *Rev. Fish. Biol. Fish.* **22**, 17–27 (2012).
23. Wouters, J., Janson, S., Lusková, V. & Olsén, K. H. Molecular identification of hybrids of the invasive gibel carp *Carassius auratus gibelio* and crucian carp *Carassius carassius* in Swedish waters. *J. Fish. Biol.* **80**, 2595–2604 (2012).
24. Tapkir, S. et al. Invasive gibel carp (*Carassius gibelio*) outperforms threatened native crucian carp (*Carassius gibelio*) in growth rate and effectiveness of resource use: field and experimental evidence. *Aquat. Conserv. Mar. Freshw. Ecosyst.* **32**, 1901–1912 (2022).
25. Li, X. Y. et al. Evolutionary history of two divergent *Dmrt1* genes reveals two rounds of polyploidy origins in gibel carp. *Mol. Phylogenet. Evol.* **78**, 96–104 (2014).
26. Luo, J. et al. Tempo and mode of recurrent polyploidization in the *Carassius auratus* species complex (Cypriniformes, Cyprinidae). *Heredity* **112**, 415–427 (2014).
27. Schlupp, I. The evolutionary ecology of gynogenesis. *Annu. Rev. Ecol. Evol. Syst.* **36**, 399–417 (2005).
28. Neaves, W. B. & Baumann, P. Unisexual reproduction among vertebrates. *Trends Genet.* **27**, 81–88 (2011).
29. Przybył, A. Sex, size and ploidy ratios of *Carassius gibelio* from Poland. *Aquat. Invasions*. **15**, 335–354 (2020).
30. Ojima, Y. & Takai, A. Further cytogenetical studies on the origin of the goldfish. *Proc. Jpn. Acad. Ser. B.* **55**, 346–350 (1979).
31. Li, X. Y. et al. Origin and transition of sex determination mechanisms in a gynogenetic hexaploid fish. *Heredity* **121**, 64–74 (2018).
32. Goto-Kazeto, R. et al. Temperature-dependent sex differentiation in goldfish: Establishing the temperature-sensitive period and effect of constant and fluctuating water temperatures. *Aquaculture* **254**, 617–624 (2006).
33. Zhu, Y. J. et al. Distinct sperm nucleus behaviors between genotypic and temperature-dependent sex determination males are associated with replication and expression-related pathways in a gynogenetic fish. *BMC Genom.* **19**, 437 (2018).
34. Ahmad, S. F. & Martins, C. The modern view of B chromosomes under the impact of high scale omics analyses. *Cells* **8**, 156 (2019).
35. Ding, M. et al. Genomic anatomy of male-specific microchromosomes in a gynogenetic fish. *PLoS Genet.* **17**, e1009760 (2021).
36. Li, X. Y. et al. Extra microchromosomes play male determination role in polyploid gibel carp. *Genetics* **203**, 1415–1424 (2016).
37. Muller, H. J. The relation of recombination to mutational advance. *Mutat. Res. Mol. Mech. Mutagen.* **1**, 2–9 (1964).
38. Hamilton, W. D., Axelrod, R. & Tanese, R. Sexual reproduction as an adaptation to resist parasites (a review). *Proc. Natl. Acad. Sci.* **87**, 3566–3573 (1990).
39. Šimková, A., Košař, M., Vetešník, L. & Vyskočilová, M. MHC genes and parasitism in *Carassius gibelio*, a diploid-triploid fish species with dual reproduction strategies. *BMC Evol. Biol.* **13**, 122 (2013).
40. Zhao, X. et al. Genotypic males play an important role in the creation of genetic diversity in gynogenetic gibel carp. *Front. Genet.* **12**, 691923 (2021).
41. Gui, J. & Zhou, L. Genetic basis and breeding application of clonal diversity and dual reproduction modes in polyploid *Carassius auratus gibelio*. *Sci. China Life Sci.* **53**, 409–415 (2010).
42. Du, W. X. et al. Gonadal temperature-sensitive gene identification in gynogenetic gibel carp (*Carassius gibelio*) with temperature-dependent sex determination. *Aquaculture* **611**, 743035 (2026).
43. Teng, J., Zhao, Y., Chen, H. J., Wang, H. & Ji, X. S. Transcriptome profiling and analysis of genes associated with high temperature-induced masculinization in sex-undifferentiated Nile tilapia gonad. *Mar. Biotechnol.* **22**, 367–379 (2020).
44. Wang, C. et al. Comparative transcriptome analysis of heat-induced domesticated zebrafish during gonadal differentiation. *BMC Genomic Data*. **23**, 39 (2022).
45. Brown-Peterson, N. J., Wyanski, D. M., Saborido-Rey, F., Macewicz, B. J. & Lowerre-Barbieri, S. K. A standardized terminology for describing reproductive development in fishes. *Mar. Coast. Fish.* **3**, 52–70 (2011).
46. Jacques, F. et al. Reproduction-associated pathways in females of gibel carp (*Carassius gibelio*) shed light on the molecular mechanisms of the coexistence of asexual and sexual reproduction. *BMC Genom.* **25**, 548 (2024).
47. Von Hofsten, J., Larsson, A. & Olsson, P. E. Novel steroidogenic factor-1 homolog (*ff1d*) is coexpressed with anti-Mullerian hormone (*amh*) in zebrafish. *Dev. Dyn.* **233**, 595–604 (2005).
48. Sandra, G. E. & Norma, M. M. Sexual determination and differentiation in teleost fish. *Rev. Fish. Biol. Fish.* **20**, 101–121 (2010).
49. Matsumoto, Y. & Crews, D. Molecular mechanisms of temperature-dependent sex determination in the context of ecological developmental biology. *Mol. Cell. Endocrinol.* **354**, 103–110 (2012).
50. Hattori, R. S., Strüssmann, C. A., Fernandino, J. I. & Somoza, G. M. Genotypic sex determination in teleosts: insights from the testis-determining *Amhy* gene. *Gen. Comp. Endocrinol.* **192**, 55–59 (2013).
51. Merchant-Larios, H., Díaz-Hernández, V. & Cortez, D. Molecular and cellular mechanisms underlying temperature-dependent sex determination in turtles. *Sex. Dev.* **15**, 38–46 (2021).
52. Hillers, K. J. & Villeneuve, A. M. Chromosome-wide control of meiotic crossing over in *C. elegans*. *Curr. Biol.* **13**, 1641–1647 (2003).
53. Ramesh, M., Malik, S. & Logsdon, J. A. Phylogenomic inventory of meiotic genes evidence for sex in *Giardia* and an early eukaryotic origin of meiosis. *Curr. Biol.* **15**, 185–191 (2005).
54. Schurko, A. M. & Logsdon, J. M. Using a meiosis detection toolkit to investigate ancient asexual scandals and the evolution of sex. *BioEssays* **30**, 579–589 (2008).
55. Patil, S. et al. Identification of the meiotic toolkit in diatoms and exploration of meiosis-specific *SPO11* and *RAD51* homologs in the sexual species *Pseudo-nitzschia multistriata* and *Seminavis robusta*. *BMC Genom.* **16**, 930 (2015).
56. Maciver, S. K. Asexual amoebae escape muller's ratchet through polyploidy. *Trends Parasitol.* **32**, 855–862 (2016).
57. Kipreos, E. T. & Pagano, M. The F-box protein family. *Genome Biol.* **1**, 3002–1 (2000).
58. Stacey, D. W. Cyclin D1 serves as a cell cycle regulatory switch in actively proliferating cells. *Curr. Opin. Cell. Biol.* **15**, 158–163 (2003).
59. Molina, J. R. & Adjei, A. A. The Ras/Raf/MAPK pathway. *J. Thorac. Oncol.* **1**, 7–9 (2006).
60. Tidyman, W. E. & Rauen, K. A. The rasopathies: developmental syndromes of Ras/MAPK pathway dysregulation. *Curr. Opin. Genet. Dev.* **19**, 230–236 (2009).
61. Goriely, A. & Wilkie, A. O. M. Paternal age effect mutations and selfish spermatogonial selection: causes and consequences for human disease. *Am. J. Hum. Genet.* **90**, 175–200 (2012).
62. Birchmeier, C., Broek, D. & Wigler, M. RAS proteins can induce meiosis in xenopus oocytes. *Cell* **43**, 615–621 (1985).
63. Cotton, L. M., O'Bryan, M. K. & Hinton, B. T. Cellular signaling by fibroblast growth factors (FGFs) and their receptors (FGFRs) in male reproduction. *Endocr. Rev.* **29**, 193–216 (2008).

64. Offen, N., Blum, N., Meyer, A. & Begemann, G. *Fgfr1* signalling in the development of a sexually selected trait in vertebrates, the sword of swordtail fish. *BMC Dev. Biol.* **8**, 98 (2008).
65. Stenberg, P. & Saura, A. Meiosis and its deviations in polyploid animals. *Cytogenet. Genome Res.* **140**, 185–203 (2013).
66. Spangenberg, V. et al. Reticulate evolution of the rock lizards: meiotic chromosome dynamics and spermatogenesis in diploid and triploid males of the genus *Darevskia*. *Genes* **8**, 149 (2017).
67. Hu, Y., Wang, B. & Du, H. A review on *Sox* genes in fish. *Rev. Aquac.* **13**, 1986–2003 (2021).
68. Han, J. et al. High temperature induced masculinization of zebrafish by down-regulation of *sox9b* and *esr1* via DNA methylation. *J. Environ. Sci.* **107**, 160–170 (2021).
69. Takada, S. & Koopman, P. Origin and possible roles of the *Sox8* transcription factor gene during sexual development. *Cytogenet. Genome Res.* **101**, 212–218 (2003).
70. Chaboissier, M. C. et al. Functional analysis of *Sox8* and *Sox9* during sex determination in the mouse. *Development* **131**, 1891–1901 (2004).
71. Yu, H. et al. The evolution and possible role of two *Sox8* genes during sex differentiation in Japanese flounder (*Paralichthys olivaceus*). *Mol. Reprod. Dev.* **86**, 592–607 (2019).
72. Yang, B. et al. *SOX8* is essential for male sexual differentiation in the Chinese soft-shelled turtle *Pelodiscus sinensis*. *Biol. Reprod.* **108**, 988–996 (2023).
73. Yu, H. et al. Genome-wide identification and transcriptome-based expression analysis of Sox gene family in the Japanese flounder *Paralichthys olivaceus*. *J. Oceanol. Limnol.* **36**, 1731–1745 (2018).
74. Barrionuevo, F. J. et al. *Sox9* and *Sox8* protect the adult testis from male-to-female genetic reprogramming and complete degeneration. *Elife.* **5**, e15635 (2016).
75. Xiao, L. et al. Comparative transcriptome analysis of diploid and triploid hybrid groupers (*Epinephelus coioides*♀ × *E. lanceolatus*♂) reveals the mechanism of abnormal gonadal development in triploid hybrids. *Genomics* **111**, 251–259 (2019).
76. Raymond, C. S., Kettlewell, J. R., Hirsch, B., Bardwell, V. J. & Zarkower, D. Expression of *Dmrt1* in the genital ridge of mouse and chicken embryos suggests a role in vertebrate sexual development. *Dev. Biol.* **215**, 208–220 (1999).
77. Marchand, O. et al. DMRT1 expression during gonadal differentiation and spermatogenesis in the rainbow trout, *Oncorhynchus mykiss*. *Biochim. Biophys. Acta*. **1493**, 180–187 (2000).
78. Ge, C. et al. *Dmrt1* induces the male pathway in a turtle with temperature-dependent sex determination. *Development dev.* https://doi.org/10.1242/dev.152033 (2017).
79. Poonlaphdecha, S. et al. Temperature induced-masculinisation in the Nile tilapia causes rapid up-regulation of both *dmrt1* and *amh* expressions. *Gen. Comp. Endocrinol.* **193**, 234–242 (2013).
80. Fernandino, J. I., Hattori, R. S., Kimura, H., Strüssmann, C. A. & Somoza, G. M. Expression profile and estrogenic regulation of anti-Müllerian hormone during gonadal development in pejerrey *Odontesthes bonariensis*, a teleost fish with strong temperature-dependent sex determination. *Dev. Dyn.* **237**, 3192–3199 (2008).
81. Shirak, A. et al. *Amh* and *Dmrta2* genes map to tilapia (*Oreochromis* spp.) linkage group 23 within quantitative trait locus regions for sex determination. *Genetics* **174**, 1573–1581 (2006).
82. Xu, S., Xia, W., Zohar, Y. & Gui, J. F. Zebrafish *dmrta2* regulates the expression of *cdkn2c* in spermatogenesis in the adult testis. *Biol. Reprod.* **88**, 14–1 (2013).
83. Yoshizawa, A. et al. Zebrafish Dmrta2 regulates neurogenesis in the telencephalon. *Genes Cells*. **16**, 1097–1109 (2011).
84. Graf, M., Teo Qi-Wen, E.-R., Sarusie, M. V., Rajaei, F. & Winkler, C. Dmrt5 controls corticotrope and gonadotrope differentiation in the zebrafish pituitary. *Mol. Endocrinol.* **29**, 187–199 (2015).
85. Johnsen, H., Tveiten, H., Torgersen, J. S. & Andersen, Ø. Divergent and sex-dimorphic expression of the paralogs of the Sox9-Amh-Cyp19a1 regulatory cascade in developing and adult Atlantic cod (*Gadus morhua* L). *Mol. Reprod. Dev.* **80**, 358–370 (2013).
86. Ahmed, S. Review of the molecular modelling studies of the cytochrome P-450 estrogen synthetase enzyme, aromatase. *Drug Des. Discov*. **15**, 239–252 (1998).
87. Kitano, T., Takamune, K., Kobayashi, T., Nagahama, Y. & Abe, S. Suppression of P450 aromatase gene expression in sex-reversed males produced by rearing genetically female larvae at a high water temperature during a period of sex differentiation in the Japanese flounder (*Paralichthys olivaceus*). *J. Mol. Endocrinol.* **23**, 167–176 (1999).
88. D'Cotta, H., Fostier, A., Guiguen, Y., Govoroun, M. & Baroiller, J. Aromatase plays a key role during normal and temperature-induced sex differentiation of tilapia *Oreochromis niloticus*. *Mol. Reprod. Dev.* **59**, 265–276 (2001).
89. Ijiri, S. et al. Sexual dimorphic expression of genes in gonads during early differentiation of a teleost fish, the nile tilapia *Oreochromis niloticus*. *Biol. Reprod.* **78**, 333–341 (2008).
90. Van Nes, S. & Andersen, Ø. Temperature effects on sex determination and ontogenetic gene expression of the aromatases *cyp19a* and *cyp19b*, and the estrogen receptors *esr1* and *esr2* in Atlantic halibut (*Hippoglossus hippoglossus*). *Mol. Reprod. Dev.* **73**, 1481–1490 (2006).
91. Pfennig, F., Standke, A. & Gutzeit, H. O. The role of *Amh* signaling in teleost fish - multiple functions not restricted to the gonads. *Gen. Comp. Endocrinol.* **223**, 87–107 (2015).
92. Rodríguez-Marí, A. et al. Characterization and expression pattern of zebrafish *anti-Müllerian hormone* (*amh*) relative to *sox9a*, *sox9b*, and *cyp19a1a*, during gonad development. *Gene Expr. Patterns*. **5**, 655–667 (2005).
93. Johnsen, H. & Andersen, Ø. Sex dimorphic expression of five *dmrt* genes identified in the Atlantic cod genome. The fish-specific *dmrt2b* diverged from *dmrt2a* before the fish whole-genome duplication. *Gene* **505**, 221–232 (2012).
94. Wang, W. et al. *Amh* dominant expression in Sertoli cells during the testicular differentiation and development stages in the olive flounder *Paralichthys olivaceus*. *Gene* **755**, 144906 (2020).
95. Gomes Fernandes, M. et al. Human-specific subcellular compartmentalization of P-element induced wimpy testis-like (PIWIL) granules during germ cell development and spermatogenesis. *Hum. Reprod.* **33**, 258–269 (2018).
96. Manna, P. R., Stetson, C. L., Slominski, A. T. & Pruitt, K. Role of the steroidogenic acute regulatory protein in health and disease. *Endocrine* **51**, 7–21 (2016).
97. Deng, Q. et al. Sex-Inclined Piwi-Interacting RNAs in serum exosomes for sex determination in the greater amberjack (*Seriola dumerili*). *Int. J. Mol. Sci.* **24**, 3438 (2023).
98. Giuili, G., Shen, W. H. & Ingraham, H. A. The nuclear receptor SF-1 mediates sexually dimorphic expression of Müllerian inhibiting substance, in vivo. *Development* **124**, 1799–1807 (1997).
99. Bollig, F. et al. Identification and comparative expression analysis of a second *wt1* gene in zebrafish. *Dev. Dyn.* **235**, 554–561 (2006).
100. Valenzuela, N., Neuwald, J. L. & Literman, R. Transcriptional evolution underlying vertebrate sexual development. *Dev. Dyn.* **242**, 307–319 (2013).
101. Zhou, T. et al. Single-molecule real-time sequencing for identifying sexual-dimorphism-related transcriptomes and genes in the Chinese soft-shelled turtle (*Pelodiscus sinensis*). *Animals* **13**, 3704 (2023).
102. Chen, R. et al. Characterization and functional analysis of the 17-beta hydroxysteroid dehydrogenase 2 (*hsd17b2*) gene during sex reversal in the ricefield eel (*Monopterus albus*). *Int. J. Mol. Sci.* **25**, 9063 (2024).
103. Erwin, D. H. The origin of animal body plans: a view from fossil evidence and the regulatory genome. *Development* **147**, dev182899 (2020).
104. Jacques, F., Baratchart, E., Pienta, K. J. & Hammarlund, E. U. Origin and evolution of animal multicellularity in the light of phylogenomics and cancer genetics. *Med. Oncol.* **39**, 160 (2022).

105. Amberg, J. J., Goforth, R. R. & Sepúlveda, M. S. Antagonists to the Wnt cascade exhibit sex-specific expression in gonads of sexually mature shovelnose sturgeon. *Sex. Dev.* **7**, 308–315 (2013).
106. Liu, Y. et al. Sexually dimorphic expression in developing and adult gonads shows an important role of gonadal soma-derived factor during sex differentiation in olive flounder (*Paralichthys olivaceus*). *Comp. Biochem. Physiol. B Biochem. Mol. Biol.* **210**, 1–8 (2017).
107. Prathibha, Y. & Senthilkumaran, B. Expression of *wnt4/5* during reproductive cycle of catfish and *wnt5* promoter analysis. *J. Endocrinol.* **232**, 1–13 (2017).
108. Schiffer, M., Von Gersdorff, G., Bitzer, M., Susztak, K. & Böttinger, E. P. Smad proteins and transforming growth factor-β signaling. *Kidney Int.* **58**, S45–S52 (2000).
109. Aguero, T. et al. Hermes (Rbpms) is a critical component of RNP complexes that sequester germline RNAs during oogenesis. *J. Dev. Biol.* **4**, 2 (2016).
110. Wilson, M. L. et al. Rbpms2 promotes female fate upstream of the nutrient sensing Gator2 complex component Mios. *Nat. Commun.* **15**, 5248 (2024).
111. Zhang, F. et al. Ski-related novel protein N (SnoN), a negative controller of transforming growth factor-beta signaling, is a prognostic marker in estrogen receptor-positive breast carcinomas. *Cancer Res.* **63**, 5005–5010 (2003).
112. Kobayashi, T. Involvement of gonadal soma-derived factor in the reproduction of teleosts. *Aquac Fish.* **9**, 417–421 (2024).
113. Shibata, Y. et al. Expression of gonadal soma derived factor (GSDF) is spatially and temporally correlated with early testicular differentiation in medaka. *Gene Expr. Patterns.* **10**, 283–289 (2010).
114. Horie, Y. et al. Androgen induces gonadal soma-derived factor, *Gsdf*, in XX gonads correlated to sex-reversal but not *Dmrt1* directly, in the teleost fish, northern medaka (*Oryzias sakaizumii*). *Mol. Cell. Endocrinol.* **436**, 141–149 (2016).
115. Kazama, H. et al. Loss of DIAPH3, a formin family protein, leads to cytokinetic failure only under high temperature conditions in mouse FM3A cells. *Int. J. Mol. Sci.* **21**, 8493 (2020).
116. Xu, K. et al. Comparative analysis of testis transcriptomes from triploid and fertile diploid cyprinid fish. *Biol. Reprod.* **92**, 95–1 (2015).
117. Pan, P. et al. Proteomic profiling of *TBC1 domain family member 21*-null sperms reveals the critical roles of TEKT 1 in their tail defects. *Dev. Dyn.* **253**, 1024–1035 (2024).
118. Li, D. Y. et al. Sperm flagellar 2 (SPEF2) is essential for sperm flagellar assembly in humans. *Asian J. Androl.* **24**, 359 (2022).
119. Grayson, P. Izumo1 and juno: the evolutionary origins and coevolution of essential sperm–egg binding partners. *R. Soc. Open. Sci.* **2**, 150296 (2015).
120. Blobel, C. P. Functional processing of fertilin: evidence for a critical role of proteolysis in sperm maturation and activation. *Rev. Reprod.* **5**, 75–83 (2000).
121. Ito, C. et al. Tetraspanin family protein CD9 in the mouse sperm: unique localization, appearance, behavior and fate during fertilization. *Cell. Tissue Res.* **340**, 583–594 (2010).
122. Jacques, F., Bolivar, P., Pietras, K. & Hammarlund, E. U. Roadmap to the study of gene and protein phylogeny and evolution - a practical guide. *PLoS One.* **18**, e0279597 (2023).
123. Dehler, C. E., Boudinot, P., Collet, B. & Martin, S. A. M. Phylogeny and expression of tetraspanin CD9 paralogues in rainbow trout (*Oncorhynchus mykiss*). *Dev. Comp. Immunol.* **146**, 104735 (2023).
124. Sebé-Pedrós, A., Roger, A. J., Lang, F. B., King, N. & Ruiz-Trillo, I. Ancient origin of the integrin-mediated adhesion and signaling machinery. *Proc. Natl. Acad. Sci.* **107**, 10142–10147 (2010).
125. Merc, V., Frolikova, M. & Komrskova, K. Role of integrins in sperm activation and fertilization. *Int. J. Mol. Sci.* **22**, 11809 (2021).
126. Wen, M. et al. Sex chromosome and sex locus characterization in goldfish, *Carassius auratus* (Linnaeus, 1758). *BMC Genom.* **21**, 552 (2020).
127. Sperry, A. O. The dynamic cytoskeleton of the developing male germ cell. *Biol. Cell.* **104**, 297–305 (2012).
128. Ma, D. D., Wang, D. H. & Yang W.-X. Kinesins in spermatogenesis. *Biol. Reprod.* **96**, 267–276 (2017).
129. Sun, M., Li, Z. & Gui, J. Dynamic distribution of Spindlin in nucleoli, nucleoplasm and spindle from primary oocytes to mature eggs and its critical function for oocyte-to-embryo transition in gibel carp. *J. Exp. Zool. Part. Ecol. Genet. Physiol.* **313A**, 461–473 (2010).
130. Kuhl, H. et al. Equilibrated evolution of the mixed auto-/allopolyploid haplotype-resolved genome of the invasive hexaploid Prussian carp. *Nat. Commun.* **13**, 4092 (2022).
131. Yuan, J. et al. Speciation of polyploid Cyprinidae fish of common carp, crucian carp, and silver crucian carp derived from duplicated *Hox* genes. *J. Exp. Zoolog. B Mol. Dev. Evol.* **314B**, 445–456 (2010).
132. Zhou, L., Wang, Y. & Gui, J. F. Genetic evidence for gonochoristic reproduction in gynogenetic silver crucian carp (*Carassius auratus gibelio* Bloch) as revealed by RAPD assays. *J. Mol. Evol.* **51**, 498–506 (2000).
133. Šimková, A., Dávidová, M., Papoušek, I. & Vetešník, L. Does interspecies hybridization affect the host specificity of parasites in cyprinid fish? *Parasit. Vectors.* **6**, 95 (2013).
134. Pakosta, T., Vetešník, L. & Šimková, A. Long temporal study of parasitism in asexual-sexual populations of *Carassius gibelio*: does the parasite infection support coevolutionary Red Queen dynamics?. *BioMed Res. Int.* **2018**, 983740 (2018).
135. Fuad, M. M. H., Vetešník, L. & Šimková, A. Is gynogenetic reproduction in gibel carp (*Carassius gibelio*) a major trait responsible for invasiveness? *J. Vertebr. Biol.* **70**, 21049 (2021).
136. Šimková, A., Vojtek, L., Halačka, K., Hyršl, P. & Vetešník, L. The effect of hybridization on fish physiology, immunity and blood biochemistry: a case study in hybridizing *Cyprinus carpio* and *Carassius gibelio* (Cyprinidae). *Aquaculture* **435**, 381–389 (2015).
137. Papoušek, I. et al. Identification of natural hybrids of gibel carp *Carassius auratus gibelio* (Bloch) and crucian carp *Carassius carassius* (L.) from lower Dyje river floodplain (Czech Republic). *J. Fish. Biol.* **72**, 1230–1235 (2008).
138. Gela, D. et al. Controlled reproduction technology of common carp (*Cyprinus carpio* L). Univ South. Bohemia České Budějovice Fac. Fish. Prot. Waters Vodňany Methodol. Ed **99**, (2009).
139. Suvarna, K. S., Layton, C. & Bancroft, J. D. *Bancroft's Theory and Practice of Histological Techniques* (Elsevier, 2019). https://doi.org/10.1016/C2015-0-00143-5.
140. Andrews, S. FastQC: a quality control tool for high throughput sequence data. (2010).
141. Dobin, A. et al. STAR: ultrafast universal RNA-seq aligner. *Bioinformatics* **29**, 15–21 (2013).
142. Wang, L., Wang, S. & Li, W. RSeQC: quality control of RNA-seq experiments. *Bioinformatics* **28**, 2184–2185 (2012).
143. Picard Toolkit. Broad Institute. (2018).
144. Okonechnikov, K., Conesa, A. & García-Alcalde, F. Qualimap 2: advanced multi-sample quality control for high-throughput sequencing data. *Bioinformatics* **32**, 292–294 (2016).
145. Ewels, P., Magnusson, M., Lundin, S. & Käller, M. MultiQC: summarize analysis results for multiple tools and samples in a single report. *Bioinformatics* **32**, 3047–3048 (2016).
146. Liao, Y., Smyth, G. K. & Shi, W. FeatureCounts: an efficient general purpose program for assigning sequence reads to genomic features. *Bioinformatics* **30**, 923–930 (2014).
147. Love, M. I., Huber, W. & Anders, S. Moderated estimation of fold change and dispersion for RNA-seq data with DESeq2. *Genome Biol.* **15**, 550 (2014).
148. Ge, S. X., Son, E. W. & Yao, R. iDEP: an integrated web application for differential expression and pathway analysis of RNA-Seq data. *BMC Bioinform.* **19**, 534 (2018).
149. The Gene Ontology Consortium. The gene ontology resource: enriching a gold mine. *Nucleic Acids Res.* **49**, D325–D334 (2021).

150. Kanehisa, M. & Goto, S. K. E. G. G. Kyoto encyclopedia of genes and genomes. *Nucleic Acid Res.* **28**, 27–30 (2000).
151. Kanehisa, M. Toward understanding the origin and evolution of cellular organisms. *Protein Sci.* **28**, 1947–1951 (2019).
152. Kanehisa, M., Furumichi, M., Sato, Y., Matsuura, Y. & Ishiguro-Watanabe, M. KEGG: biological systems database as a model of the real world. *Nucleic Acids Res.* **53**, D672–D677 (2025).
153. Sherman, B. T. et al. DAVID: a web server for functional enrichment analysis and functional annotation of gene lists (2021 update). *Nucleic Acids Res.* **50**, W216–W221 (2022).
154. Bairoch, A. The universal protein resource (UniProt). *Nucleic Acids Res.* **33**, D154–D159 (2004).
155. Bradford, Y. M. et al. Zebrafish information network, the knowledgebase for *Danio rerio* research. *Genetics* **220**, iyac016 (2022).
156. Safran, M. et al. GeneCards Version 3: the human gene integrator. Database baq020–baq020 (2010). (2010).
157. Schedina, I. M., Groth, D., Schlupp, I. & Tiedemann, R. The gonadal transcriptome of the unisexual Amazon molly *Poecilia formosa* in comparison to its sexual ancestors, *Poecilia mexicana* and *Poecilia latipinna*. *BMC Genom.* **19**, 12 (2018).
158. Vandesompele, J., Preter, K. D., Roy, N. V. & Paepe, A. D. Accurate normalization of real-time quantitative RT-PCR data by geometric averaging of multiple internal control genes. *Genome Biol.* 3, research0034.1-0034.11 (2002).
159. Ye, J. et al. Primer-BLAST: A tool to design target-specific primers for polymerase chain reaction. *BMC Bioinform.* **13**, 134 (2012).
160. Livak, K. J. & Schmittgen, T. D. Analysis of relative gene expression data using real-time quantitative PCR and the $2^{-\Delta\Delta C}{}_{T}$ Method. *Methods* **25**, 402–408 (2001).

## Acknowledgements

We thank Kristýna Voříšková and Kristína Křížová for their technical help in the molecular laboratory. Core Facility Genomics CEITEC MU, supported by the NCMG research infrastructure (LM2023067 funded by MEYS CR), and Core Facility Bioinformatics CEITEC MU are gratefully acknowledged for their assistance with obtaining scientific data presented in this paper. We also kindly thank Matthew Nicholls for English revision of the final draft. The study was funded by the Czech Science Foundation, Project No. 22–27023S.

## Author contributions

Conceptualization: AŠ, FJ, Data curation: FJ, AŠ, ID, NB, Formal analysis: FJ, AŠ, NB, Funding acquisition: AŠ, Investigation: FJ, AŠ, LV, ID, Methodology: AŠ, FJ, Project administration: AŠ, Supervision: AŠ, Validation: FJ, AŠ, Visualization: FJ, ID, Writing – original draft: FJ, Writing – review & editing: FJ, AŠ, ID, LV, NB.

## Declarations

## Competing interests

The authors declare no competing interests.

## Ethics approval and consent to participate

The research was undertaken in line with the ethical requirements of the Czech Republic. The maintenance and care of experimental fish, as well as the method of fish killing complied with legal requirements in the Czech Republic – specifically, § 6, 7, 9 and 10 regulation No. 419/2012 about the care, breeding and use of experimental animals. The experiment was approved by the Animal Care and Use Committee at the Faculty of Science, Masaryk University in Brno, Czech Republic following the approval document n. MSMT-30071/2022-5 by the Ministry of Education, Sports and Youth. The study was funded by the Czech Science Foundation, All experimental procedures involving animals were conducted in accordance with the ARRIVE guidelines (https://arriveguidelines.org). All methods were performed in accordance with the relevant guidelines and regulations Project No. 22–27023S.

## Additional information

**Supplementary Information** The online version contains supplementary material available at https://doi.org/10.1038/s41598-025-27347-5.

**Correspondence** and requests for materials should be addressed to F.J. or A.Š.